Excitonic molecules in semiconductors

V. D. Kulakovskiĭ, V. G. Lysenko, and V. B. Timofeev

Institute of Solid-State Physics of the Academy of Sciences of the USSR, Chernogolovka (Moscow district)
Usp. Fiz. Nauk **147**, 3–47 (September 1985)

Great progress has been made in recent years in experimental studies of excitonic molecules, both in direct-band and indirect-band semiconductors. The exciton systems in these semiconductors differ substantially. In direct-band semiconductors with dipole-allowed optical transitions, the direct-recombination times are extremely small. Consequently the processes of binding of excitons into excitonic molecules and their decay occur under strongly nonequilibrium conditions. Hence one can obtain the fundamental information on biexcitons in these semiconductors by nonlinear optical methods. This review discusses the processes on which the various methods are based: two-photon resonance excitation of biexcitons, induced one-photon conversion of an exciton into a biexciton, two-photon resonance Raman scattering involving biexciton states, etc., and their application to studying biexcitons with the example of CdS. Problems of bistability involving biexcitons are also briefly discussed. In indirect semiconductors, where recombination occurs with the emission of a phonon, the lifetimes of excitons are large, and quasiequilibrium can be established in the exciton system. Under these conditions the information on the properties of the molecules is obtained by analyzing their radiative-decay spectra. The problem of detecting biexcitons in indirect semiconductors, radiative decay of molecules, and the effect on their stability of external electric, strain, and magnetic fields are discussed in detail with the examples of Si and Ge. Also the results of investigating the quantum statistical behavior of a dense gas of spin-oriented excitons (in a magnetic field under conditions in which the biexcitons are destabilized) are briefly presented (using the example of uniaxially compressed germanium), and the question of the possibility of their Bose condensation is discussed.

TABLE OF CONTENTS

1. INTRODUCTION

The possibility in principle of binding in vacuo of four light particles (two electrons and two positrons) by Coulomb forces to form a neutral molecule was first shown by Hylleraas and Ore[1,2] using variational calculations. Their calculations implied that such a four-particle complex is stable against dissociation into two positronium atoms. A close analog of the positronium molecule in semiconductors is the excitonic molecule—the EM (or biexciton)—a bound complex of two electrons and two holes. The concept of a biexciton in solid-state physics was introduced by Lampert[3] and independently by Moskalenko.[4] Progress in experimental studies of properties of EMs has been most evident in recent years, both in semiconductors with a direct gap (see, e.g., the reviews of Hanamura, Haug, *et al.*[5] and Grun *et al.*[6]) and in indirect-band semiconductors (see, e.g., Ref. 7).

 0038-5670/85/090735-27$01.80

In contrast to ordinary gases, the electron-hole gas in semiconductors (electrons, holes, excitons, molecules, etc.) is in principle a nonequilibrium system owing to recombination processes. In direct-band semiconductors, where the optical interband transitions are dipole-allowed and the direct recombination times are extremely small (for gap widths $E_g > 1$ eV these times are on a nanosecond scale), the processes of binding into excitonic molecules and their decay occur under strongly nonequilibrium conditions, both with respect to the phonon system and among the components of the electron-hole system itself. Hence nonlinear optical methods have been developed for experimental study of the properties of biexcitons in these crystals, and have proved most effective under the conditions of this nonequilibrium. They include two-photon resonance excitation of biexciton,[8] induced one-photon conversion of an exciton into a biexciton,[9,10] and also two-photon resonance Raman scattering *(or hyper-Raman scattering) involving biexcitonic states.*[11] The effectiveness of these processes in direct-band semiconductors involves the gigantic value of the nonlinear susceptibility under conditions of two photon resonance with the corresponding biexcitonic state. The recently started studies of nonlinear effects in multiwave mixing and bistability involving biexcitons[12] stem from this.

The application of the cited methods of nonlinear optics in indirect-band semiconductors is less effective, owing to the small probability of optical transitions. In these semiconductors recombination is indirect in character, with participation of a phonon that carries away the Brillouin momentum. Hence they are distinguished by long times (e.g., in Si and Ge the recombination times are on a microsecond scale). We can naturally expect that the formation and decay of excitonic molecules in indirect-band semiconductors with such long recombination times will occur under quasiequilibrium conditions, even at relatively low exciton densities and low enough temperatures. Hence one can extract valuable information on the properties of EMs in these materials by analyzing their radiative-decay spectra.

Up to now, the properties of EMs in uniaxially deformed crystals of Si and Ge have been given the most rounded study. Therefore this review will mainly employ the results of studies of biexcitons in these semiconductors. In discussing the nonlinear-optical methods of studying biexcitonic states in semiconductors having a direct gap, we shall mainly employ the results for CdS, taking into account the relative simplicity of the energy spectrum (nondegenerate bands) in these crystals and the sufficiently high accuracy of the information on the needed experimental parameters.

There is a very extensive bibliography on the topic being discussed. The authors apologize in advance if any of the studies have remained uncited in this review.

2. BINDING ENERGY OF EXCITONIC MOLECULES

In semiconductors the ratio of the effective masses m_e of the electron and m_h of the hole is much larger than the ratio of masses of a free electron and a proton. In this regard, the question has arisen of the stability of EMs against dissociation into two excitons for an arbitrary value of the parameter $\sigma = m_e/m_h$.

When the effective masses of the electron and the hole do not differ strongly, the problem of four-body stability lacks a small parameter in which one can perform an expansion. Therefore the adiabatic approximation widely employed in molelcular spectroscopy is inapplicable here. In other words, when $m_e \sim m_h$, the amplitude of the zero-point vibrations proves to be on the scale of the molecule itself. Hence the very concept of "equilibrium nuclear coordinates" loses meaning.

In the limit $\sigma = 1$, the problem of the stability of EMs is quite comparable to the problem of the positronium molecule, which was first solved by Hylleraas and Ore.[1,2] Under conditions in which $m_e = m_h$, from considerations of the symmetry of the problem the attractive potential proves maximal when both the electrons and the holes exist in singlet states. *However, a stable molecular state does not arise* for the singlet wave function taken in the Heitler-London form. Hylleraas and Ore proposed using a wave function in the form[1,2]

$$\Psi_{HO} = 2\exp\left[-\tfrac{1}{2}\alpha\,(r_{1a}+r_{1b}+r_{2a}+r_{2b})\right] \times\cosh\left[\tfrac{1}{2}\beta\alpha\,(r_{1a}-r_{1b}-r_{2a}+r_{2b})\right], \quad (1)$$

Here the subscripts 1, 2, and a, b correspond to electrons and holes, and α and β are the parameters being varied. By using variational calculations on the wave function of (1), it was found that the binding energy of the positronium molecule amounts to only 0.017 of the Rydberg value Ry of the positronium atom. Such a small value of the binding energy as compared with the hydrogen molecule H_2 involves the fact that the contribution of the kinetic energy of the relative motion inside the molecule increases substantially, owing to the closeness of the masses m_e and m_h.

The binding energy Δ_M of EMs in semiconductors having different structures of the energy bands has been calculated in Refs. 13–17. In the variational calculations the wave function is usually selected in the form of the product of the Hylleraas-Ore function (Ψ_{HO}) and a shell function for the holes $F(R_h)$:

$$\Psi = \frac{\Psi_{HO}(\mathbf{r})}{S(R_h)}\,F(R_h). \quad (2)$$

Here we have $S^2(R_h) \equiv \int \Psi^2_{HO}(\mathbf{r})\,d^3r$, while R_h characterizes the distance between the holes. In the limit as $\sigma \to 1$, with $F(R_h)$ in Eq. (2) replaced by a δ-function, one obtains a trial function that has previously been used for variational calculations of the H_2 molecule.[18] In this limit, the variational calculations yield the value for the ratio $\Delta_M/\mathrm{Ry} = 0.3$, whereas the exact result is 0.35. In the limit $\sigma = 1$ we have $F(R_h) = 1$, and the wave function of (2) coincides with the Hylleraas-Ore function for the positronium molecule. The variation of the energy of the ground state $E_M(\sigma)$ was found by using the standard variational procedure—minimization of the mean value of the Hamiltonian for a trial wave function of the form of (2). The binding energy of an EM is determined with respect to dissociation to two free excitons, namely, $\Delta_M = -E_M - 2\mathrm{Ry}$.

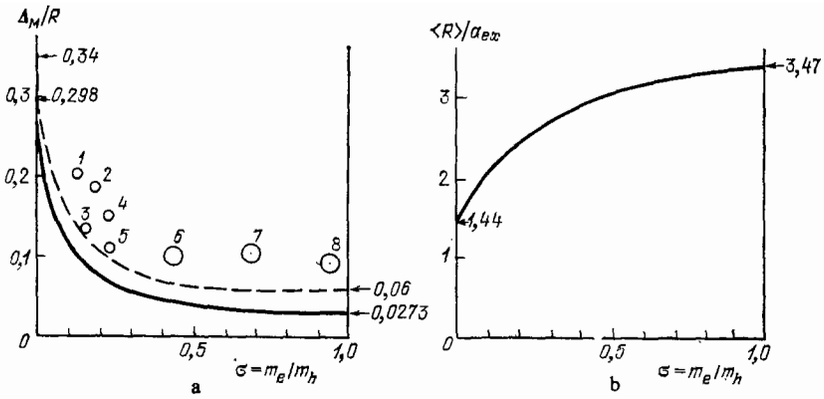

FIG. 1. Dependence of the binding energy of EMs (a) and of the ratio of the mean distance between the holes in an EM (b) on the ratio of effective masses of the electron and the hole. Solid lines—calculation by the variational method,[13] dashed line—calculation by the Monte-Carlo method using Green's functions.[17] Circles—experiment: 1—CdS,[5] 2—CuBr,[5] 3—ZnTe,[5] 4—CuCl,[5] 5—ZnSe,[5] 6—Ge $\langle\sim 100\rangle$,[30] 7—Si $\langle 100\rangle$,[35] 8—Si.[44]

The theoretical analysis of the $\Delta_M(\sigma)$ relationship showed that: 1) $\Delta_M(\sigma)$ is symmetric with respect to $\sigma = 1$,[15] 2) Δ_M decreases monotonically in the region $0 < \sigma < 1$,[15] and 3) when $\sigma \to 1$, we have $\partial\Delta_M/\partial\sigma \to 0$.[19] The results of the variational calculation of $\Delta_M(\sigma)$ are shown in Fig. 1.

The Monte Carlo method and the Green's-function formalism have been used[17] for calculating the binding energy of EMs, as based on the formal analogy between the Schrödinger equation and the diffusion equation. The electrons and holes were treated on a uniform basis. The results of the calculation are also presented in Fig. 1 (curve 2). We see from Fig. 1 that, in contrast to the variational calculations, the given method yields correct values of Δ_M as $\sigma \to 0$ ($\Delta_M \to 0.35$ Ry). Further, throughout the region of values of σ ($0 < \sigma < 1$), the calculation employing the Monte-Carlo method and the Green's-function formalism yields appreciably larger values of Δ_M than the variational calculation does[14]; as $\sigma \to 1$ the discrepancy becomes as much as a factor of two. As we shall show below, the calculations employing the Monte-Carlo method and the Green's-function formalism yield values of Δ_M that agree considerably better with the experimental values than those calculated by the variational method.

The hydrogen molecule is a rather compact structure: the distance between the two protons amounts to only $1.44a_H$, where a_H is the Bohr radius of the hydrogen atoms. As the mass ratio m_e/m_h increases, the kinetic energy of the holes increases. This leads to their delocalization and to an increase in the mean interparticle distance $\langle R_h\rangle$ between them, as calculated by the formula:

$$\langle R_h\rangle = \int \Psi^2 R_h \, d^3r \left(\alpha \int \Psi^2 \, d^3r\right)^{-1}. \qquad (3)$$

A calculation of $\langle R_h\rangle$ as a function of the parameter σ has been performed in Ref. 13. The result of the calculation is illustrated by Fig. 1, from which we see that the ratio $\langle R_h\rangle/a_{ex}$, where a_{ex} is the Bohr radius of the exciton, increases monotonically from 1.44 to 3.47. Thus, in the general case an excitonic molecule is a more open structure than a hydrogen molecule.

Several theoretical groups have studied the effect of the anisotropy of effective masses of holes (and electrons) on the magnitude of the binding energy of an excitonic molecule.[14,15] They have found that the binding energy of an EM depends weakly on the anisotropy parameter for the most typical semiconductor structures $\gamma_{e,h} = m_\perp^{e,h}/m_\parallel^{e,h}$. In the general case it tends to decrease with increasing anisotropy of the masses.

Finally, Ref. 20 has also examined the question of the influence of complex structure of the band spectrum on the energy of the ground state of the excitonic molecule. Thus, in direct-band semiconductors having the sphalerite structure, the conduction band at the Γ-point is simple and has the symmetry Γ_6, while the valence band is fourfold degenerate with respect to spin and has the symmetry Γ_8. In this case two types of excitons arise with the angular momenta $J_{ex} = 1(\Gamma_5)$ and $J_{ex} = 2(\Gamma_3 + \Gamma_4)$. The triplet state of the exciton with $J_{ex} = 2$ is optically inactive. One can choose as the basis spin functions of the EM the products of the states of two electrons with $J_e = 0$ and the states of two holes with $J_h = 0$ and $J_h = 2$, namely: $|J_M, m_M\rangle = |0,0\rangle_e |J_h, m_h\rangle_h$, where $J_M = J_h = 0$; 2. Then one can write the wave function of the EM in the form

$$|\Psi_M(J_M, m_M)\rangle = \frac{1}{\sqrt{V}} \exp(i\mathbf{k}R_0)\, \Psi(\mathbf{r}_{1a}, \mathbf{r}_{2b}, \mathbf{R}_0)|J_M, m_M\rangle. \qquad (4)$$

Here $\mathbf{R}_0$ is the coordinate of the center of mass of the molecule. Within the framework of the effective-mass approximation, the molecular states of the type of (4) are sixfold degenerate and split into three terms Γ_1, Γ_3, and Γ_5 upon taking the exchange interaction into account. The effects of the exchange interaction can appreciably affect the energy of the ground state of the EM. A striking example is the Cu_2O crystal, where a bound molecular orbital does not arise, owing to the effects of the exchange interaction, and EMs are unstable.[20] In the indirect semiconductors Si and Ge the influence of the exchange interaction on the binding energy of an EM is negligibly small, owing to the large radius of the Bohr orbits.

3. EXCITONIC MOLECULES IN SEMICONDUCTORS WITH AN INDIRECT FORBIDDEN BAND (SI AND Ge)

a) Radiative decay of EMs in uniaxially compressed crystals of Si and Ge

The most direct method of detecting and studying the properties of EMs is to analyze their radiative-recombination spectra. Owing to the strong electron-hole (e–h) pair

correlation in EMs, the most likely process of radiative decay of an EM proves to be the recombination of one e–h pair with emission of a photon and creation of a recoil exciton. In indirect semiconductors this process is accompanied by simultaneous emission of a phonon that carries away the Brillouin quasimomentum. The corresponding reaction is written in the form

$$\text{Em} \rightarrow \text{photon} + \text{phonon} + \text{exciton}. \qquad (5)$$

The first attempts to detect radiative annihilation of EMs were made in the indirect semiconductors Si and Ge. Owing to the possibility of preparing Si and Ge with a very low concentration of shallow impurities, one can avoid in these crystals the complications involving the presence of intense emission from exciton-impurity complexes, which have a substantially larger binding energy than EMs do.[3] The studies along this line were stimulated by the well-known work of Haynes,[21] who discovered a new radiative channel in pure silicon at large excitation densities of excitons. However, it was shown later that the phenomenon that he discovered involves the condensation of excitons into a dense metallic electron-hole liquid.[22–24] Owing to the strong degeneracy of the electron and hole bands, the binding energy φ of the electron hole liquid in Si and Ge crystals proves to be very large: $\varphi \sim 0.5$ Ry,[24] whereas the binding energy of an EM, as was discussed above, lies within the limit of 0.1 Ry. Owing to the relatively small binding energy of EMs in Si and Ge, the partial fraction of EMs in the nonequilibrium e–h gas proves to be small, even near the threshold for condensation to an electron-hole liquid. Estimates of the partial fraction of EMs in the gas phase performed within the framework of the principle of detailed balancing yield values for the ratio of concentrations of molecules (n_M) and of excitons (n_{ex}) $n_M/n_{ex} \approx 10^{-2}$–$10^{-3}$. Hence it becomes understandable why it has not been possible for a long time to detect EM emission in undeformed Si and Ge, despite intensive searches for this radiative channel.

One can appreciably increase the partial fraction of EMs, and thus create a more preferable situation for their experimental detection by uniaxially deforming the crystals.[1)] In uniaxial deformation of Si and Ge crystals, the binding energy of the electron-hole liquid decreases owing to the increased contribution of the kinetic energy because of the removal of orbital degeneracy in the electron and hole bands.[24,26–28] Consequently the density of the gas phase increases, and hence also the partial fraction of EMs, since we have $n_M/n_{ex} \sim n_{ex}$. The most favorable situation exists in crystals of Si and Ge compressed along an axis close to ⟨100⟩, for which the binding energy of the fluid declines by a factor of four or five, while the density of the gas phase increases by more than an order of magnitude.[27,29,30] The binding energy of EMs, just like the excitonic Rydberg energy, varies little upon removing the degeneracy of the bands. In the radiative recombination of an EM, part of its energy is transferred to the remaining exciton. Hence the emission line of an EM must lie on the long-wavelength side of the emission line of free excitons (FEs). Such a line (M) has been detected by studying the kinetics of recombination-radiation spectra of high-purity silicon crystals (concentration of residual shallow impurities less than 10^{12} cm^{-3}) strongly compressed along the ⟨100⟩ axis (Si ⟨100⟩) (pressure $P < 200$ MPa) under pulsed excitation yielding a mean density of e–h pairs $\bar{n} \sim 10^{17}$ cm^{-3} (Fig. 2a).[31] After decay of the emission from the electron-hole liquid (line L), the form of the long-wavelength edge of the line M remains unchanged. As one should expect, the spacing between the maxima of the M and FE lines does not depend on the magnitude of the deformation, and amounts to about 2 meV in Si.

The molecular nature of the M line is confirmed by experiments performed with strongly uniaxially deformed crystals of Si ($P > 500$ MPa) under conditions of steady-state bulk excitation.[29] Figure 2b illustrates the change in the emission spectra of strongly compressed Si ⟨100⟩ crystals upon increasing the excitation density. At low excitation densities one observes in the spectrum the emission from free excitons (FE line) and those bound to residual acceptors (BE line). The channel associated with recombination of exciton-impurity complexes is rapidly saturated. Here the

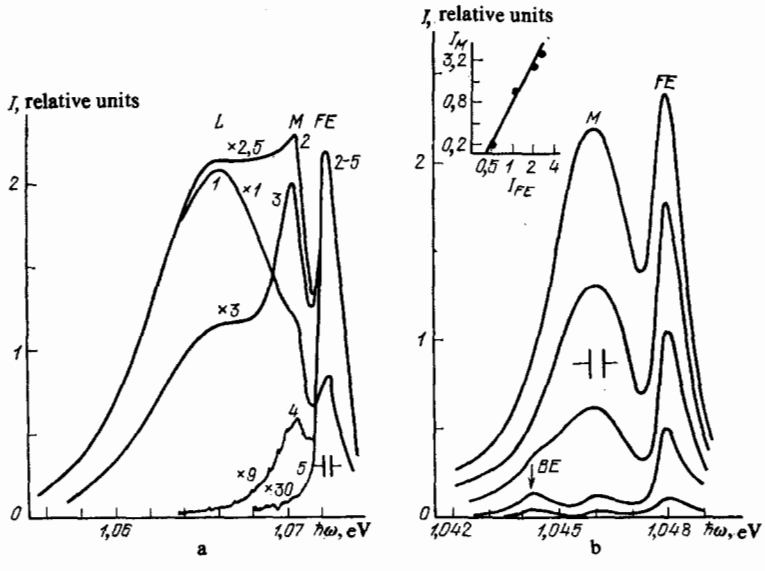

FIG. 2. Emission spectra of uniaxially compressed Si ⟨100⟩ crystals at $T = 1.8$ K with different excitation conditions. a—Pulsed excitation ($\bar{n} \sim 3 \times 10^{17}$ cm^{-3}; spectra 1–5 correspond to delays with respect to the excitation pulse of respectively 0; 0.25; 0.35; 0.7; and 1.1 μs[31]); b—bulk steady-state excitation; the mean density $\bar{n}$ varies from $\sim 10^{14}$ to 10^{15} cm^{-3}; the inset shows the dependence of the emission intensity of EMs on the intensity of emission of free excitons on a logarithmic scale; the straight line corresponds to the relationship $I_M \propto I_{FE}^{2}$.[29]

emission line of EMs appears in the spectrum. As one should expect from the molecular origin of this line, its intensity increases in proportion to the square of the intensity of the exciton line (inset in Fig. 2b). At greater densities ($\bar{n} > 10^{15}$ cm^{-3}), the intensity of the M line, just like that of the FE line, saturates owing to the condensation of the exciton gas and the EMs into an electron-hole liquid.

In Ge crystals the experimental detection of EMs involves additional difficulties, first, because of the smaller scale (by a factor of ~ 5) of the binding energy of excitons into EMs, and second, because of the greater stability of the (e–h) liquid owing to the strong anisotropy of the bands.[29] Thus, in Ge compressed along the ⟨111⟩ axis ($P \sim 150$ MPa), the binding energy of the e–h liquid still remains rather large ($\varphi \sim 0.27$ Ry), despite the complete removal of the degeneracy of the bands.[32] Only when one deforms Ge along an asymmetric direction close to ⟨100⟩ ($\mathbf{P} \parallel \langle 100 \rangle$) (Ge⟨$\sim 100$⟩), for which the anisotropy of the valence band proves relatively small, and hence the density of hole states is minimal, can one decrease the binding energy of the electron-hole liquid to ~ 0.1 Ry.[33] Under these conditions one observes an intense emission line of EMs in the emission spectrum of Ge[30,34] (Fig. 3). Its intensity is proportional to the square of the intensity of the FE line, as one sees well by comparing the recordings of spectra using 100% and 13% modulation of the intensity of the exciting laser. The found value of the power-law exponent of the relationship $I_M \sim I_{FE}^k$ ($k = (I_M/I_{Fe})_{dif}/(I_M/I_{FE})_{int}$) amounts to 1.9 ± 0.1.

Figure 4 shows the result of comparing the form of the M and FE lines in Ge(~ 100) and Si⟨100⟩, as recorded for identical ratios kT/Ry and intensities of the M and FE lines. The inset in this diagram shows the emission spectra of EMs

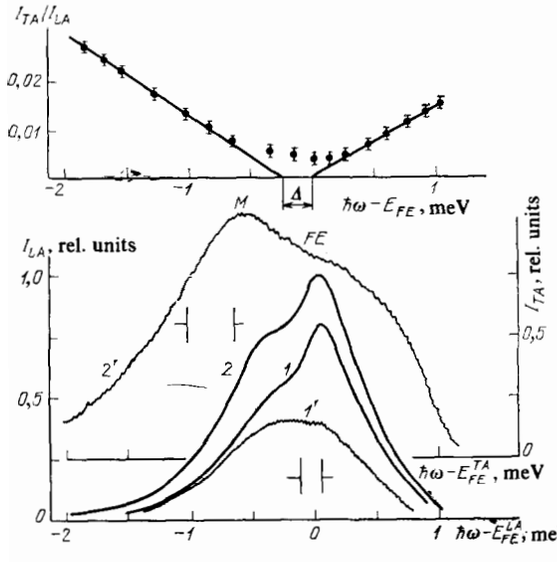

FIG. 3. Emission spectra of excitons and EMs in Ge ⟨~ 100⟩ at $T = 1.8$ K with emission of LA- and TA-phonons.[30] The LA spectra 1 and 1′ are recorded at 100 and 13% modulation of the intensity of the exciting light ($W = 20$ W/cm^2): 1—integral, and 1′—differential spectra (magnification × 6). the TA (2′) and LA (2) spectra are recorded at $W = 25$ W/cm^2; the TA spectrum is magnified × 42; the ratio of the intensities of the TA and LA components is shown in the upper part of the diagram.

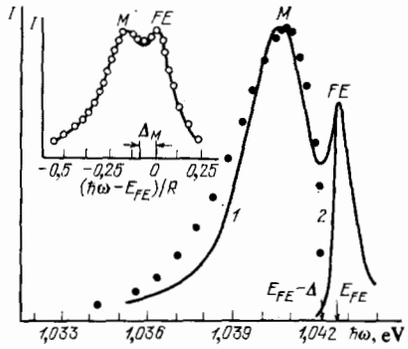

FIG. 4. Comparison of the experimental contour of the EM emission line in Si ⟨100⟩ with the calculated contour (symbols) and with the contour of the EM emission line in Ge ⟨~ 100⟩ (inset). The emission spectra 1 and 2 of Si are recorded at $T = 1.8$ K and at excitation densities $\bar{n} \approx 3 \times 10^{15}$ cm^{-3} and 3×10^{13} cm^{-3} respectively.[29] The emission spectra of Si (circles) and Ge (solid line) shown in the inset are drawn for convenience of comparison at identical ratios $I_M/I_{FE} = 1$ and $kT/\text{Ry} = 0.05$.[42]

and excitons in Ge at $T = 1.5$ K $= 0.05R$ (Ge) and in Si ⟨100⟩ at $T = 7$ K $= 0.05$ Ry (Si). The energy scale is dimensionless in units of the corresponding Rydbergs. The essential point is that one employs no adjustable parameters in such a comparison. The good agreement of the shape of the emission spectra for Si and Ge confirms the identical (molecular) nature of the M line in these crystals.

b) Shape of the emission spectrum of EMs in indirect annihilation

In the indirect radiative decay of EMs, the corresponding emission line must have a finite width, even at $T = 0$ K, since part of the energy of the EM is transferred upon recombination to the remaining recoil exciton. One can estimate the width of the emission line of EMs from the following considerations.[31] Since the wave functions of the exciton and the EM have dimensions of the order of the Bohr radius of an exciton, a_{ex}, the matrix element M of the radiative transition must be substantial in the region of wave vectors of the recoil exciton $k_{ex} \lesssim a_{ex}^{-1}$. Hence the energy that the recoil exciton carries away upon recombination of the EM lies in the range

$$\frac{\hbar^2 k_{ex}^2}{2M_{ex}} \lesssim \frac{\hbar^2}{2M_{ex}a_{ex}^2} = \frac{m_{ex}}{M_{ex}} \text{ Ry}. \qquad (6)$$

Here m_{ex} and M_{ex} are respectively the reduced and translational effective masses of the excitons. Estimates by Eq. (6) yield values of the width of the M line of about 3 meV in Si and 0.5 meV in Ge, which agree well with the experimental values. It is also evident from the arguments presented above that only the "violet" edge of the M line should be sensitive to the temperature at low enough temperatures $kT \gtrsim (m_{ex}/M_{ex})R$ (owing to the change in the energy distribution of the EMs), while the shape of the "red edge," which is determined by recoil effects, should change little. This conclusion agrees well with the results of experimental studies of the influence of the temperature on the form of the M line performed in Refs. 31, 35, and 36.

The fact that the "red" edge of the M line involves recoil effects can be demonstrated directly for Ge. A group analysis implies that in Ge the transitions with emission of LA-

phonons are allowed, while those with emission of TA-phonons are forbidden in the zero order in $\mathbf{k}$.[25] Therefore, in the recombination of excitons with creation of a TA-phonon, an extra factor appears in the matrix element that is proportional to their quasimomentum,[37] while the spectral dependences of the TA- and LA-components of the exciton emission line are related by:

$$I_{\mathrm{FE}}^{\mathrm{TA}}(E) \sim E I_{\mathrm{FE}}^{\mathrm{LA}}(E). \tag{7}$$

Here the energy $E \sim \mathbf{k}_{\mathrm{ex}}^2$ is measured from the low-frequency boundary of the spectrum ($E = 0$ corresponds to emission of an exciton at rest). In the case of radiative decay of an EM, the quasimomentum is carried away by the recoil exciton. Therefore, at $T \approx 0$ K the ratio of the intensities of the TA- and LA-components must increase with decreasing energy of the emitted quantum:

$$I_{\mathrm{M}}^{\mathrm{TA}}(E+\Delta_{\mathrm{M}}) \sim (-E-\Delta_{\mathrm{M}})\, I_{\mathrm{M}}^{\mathrm{LA}}(E+\Delta_{\mathrm{M}}). \tag{8}$$

A comparison of the emission spectra of excitons and EMs with emission of TA- and LA-phonons is shown in Fig. 3 (curves **2'** and **2**, respectively).[30] The upper part of the diagram presents the ratio of intensities $I^{\mathrm{TA}}/I^{\mathrm{LA}}$. In agreement with Eqs. (7) and (8), we see that the ratio $I^{\mathrm{TA}}/I^{\mathrm{LA}}$ increases in the recombination of excitons with increasing $\hbar\omega$ in proportion to their thermal energy. In recombination of EMs it increases with decreasing $\hbar\omega$ in proportion to the recoil energy of the exciton ($-E-\Delta_{\mathrm{M}}$). Near the violet edge of the M line Eq. (8) breaks down owing to the thermal energy distribution of the EMs.

For an analytical description of the shape of the emission line of an indirect biexciton, one must know the matrix element of the transition. A detailed calculation of the annihilation amplitude of biexcitons has been performed in Ref. 29. The matix element of the transition was found in the second order of perturbation theory, and after transformations was converted to the form

$$M(\mathbf{P}|\mathbf{p}_{\mathrm{e}}\ \mathbf{q}) \sim \int \mathrm{d}^3r\, \mathrm{d}^3r_{\mathrm{e}}\, \mathrm{d}^3r_{\mathrm{h}}\, \Psi^{\mathbf{P}}(\mathbf{r}_{\mathrm{e}}\ \mathbf{r}_{\mathrm{e}}|\mathbf{r},\ \mathbf{r}_{\mathrm{h}}) \times \exp(-i\mathbf{q}\cdot\mathbf{r})\, \psi^{*\mathbf{p}}(\mathbf{r}_{\mathrm{e}}|\mathbf{r}_{\mathrm{h}}). \tag{9}$$

Here $\Psi^{\mathbf{P}}$, $e^{-i\mathbf{q}\cdot\mathbf{r}}$, and $\psi^{\mathbf{p}}$ are the wave functions of the molecule, the phonon, and the exciton. This formula generalizes the well known formula of Elliott[38] for the annihilation amplitude of an exciton, which is proportional to $\psi_{\mathrm{ex}}(0)$, and also has a perspicuous physical meaning. We see from Eq. (9) that this is the amplitude of the probability of finding in the biexciton one of the electrons and one of the holes at one site, while the other—electron and hole—form an exciton with the wave function $\psi^{\mathbf{p}}$. The authors of Ref. 29 calculated the matrix element $\mathbf{M}(\mathbf{P}|\mathbf{p}, \mathbf{q})$ by numerical integration of Eq. (9) using the wave function of the biexciton corresponding to the best of the known variational approximations.[14] As was expected, practically the entire function $\mathbf{M}(\mathbf{P}|\mathbf{p}, \mathbf{q})$ is concentrated in a region $pa_{\mathrm{ex}}/\hbar < 1$.

If we neglect the phonon dispersion, then we can derive the following expression for the probability of emitting light at the frequency ω:

$$I(\hbar\omega) \sim \int \mathrm{d}^3\mathbf{P}\, \mathrm{d}^3\mathbf{p}\, \exp\left(-\frac{\mathbf{P}^2}{8M_{\mathrm{ex}}kT}\right) M^2\left(\left|\mathbf{p}-\frac{1}{2}\mathbf{P}\right|\right) \times \delta(E_{\mathrm{M}}^{\mathbf{P}} - E_{\mathrm{ex}}^{\mathbf{p}} - \hbar\omega - \hbar\Omega_{\mathbf{q}}). \tag{10}$$

At temperatures so low that the mean thermal momentum $\mathbf{P}$ of the biexciton satisfies the inequality $(1/\hbar)\langle P\rangle a_{\mathrm{ex}} \ll 1$, we see from (10) that the shape of the line is given by the expression

$$I(\hbar\omega) \sim |\mathbf{p}|\, M^2(\mathbf{p}). \tag{11}$$

Here we have $\mathbf{p}^2 = 4M_{\mathrm{ex}}(E_{\mathrm{ex}} - \hbar\omega - \Delta_{\mathrm{M}} - \hbar\Omega_{\mathrm{q}})$. Figure 4 shows the experimental contour of the biexciton emission line in Si at $T = 1.8$ K and an approximation of the contour calculated by Eq. (10). In constructing it, we have adopted a binding energy of an exciton of 12 meV, $a_{\mathrm{ex}} = 52.5$ Å, and $\Delta_{\mathrm{M}} = 0.4$ meV.[29] The agreement between theory and experiment seems satisfactory, and all the more so if we allow for the fact that no adjustable parameters were used in this approximation. Here it is important to stress that both the shape of the line and the binding energy are determined unambiguously by the wave function of the biexciton. Hence they are not independent quantities. Therefore it is difficult to determine the binding energy of an excitonic molecule to high accuracy by analysis of the line shape.

c) Binding energy of EMs in Si and Ge (experimental methods)

One can employ the following two methods to determine the binding energy of an EM: first, one can extract the value of Δ_{M} from analyzing the spectral arrangment of the emission lines of EMs and free excitons, and second, one can determine it by measuring the temperature variation in the relative intensities of these lines (proportional to the concentration). Neither method lacks faults. Thus, at a finite temperature the EM emission line does not have a sharply defined short-wavelength boundary corresponding to a transition from the ground state of the EM (with $\mathbf{P} = 0$) to the ground state of a free exciton (with $\mathbf{p} = 0$). Yet the second method is valid only in the presence of thermal equilibrium between excitons and EMs.

Cho[39] has proposed a simple model description for the amplitude of indirect annihilation of EMs of the following form:

$$M(\mathbf{P}|\mathbf{p}) \sim \left[\left(\frac{1}{2}\mathbf{P}-\mathbf{p}\right)^2 + a_{\mathrm{M}}^{-2}\right]^{-2}. \tag{12}$$

Upon choosing the parameter $a_{\mathrm{M}} \approx 1.2a_{\mathrm{ex}}$, we can satisfactorily describe the "red" tail of the emission line M. By using this approximation of the contour of the EM emission line, it has been found[31,35,36,40] that the binding energy of EMs in Si ⟨100⟩ amounts to 1.3–1.4 meV ≈ 0.1 Ry. However, in the light of what we have presented in the previous section, it is not clear what the true error is in estimating the binding energy of EMs on the basis of using Eq. (12).

References 29, 35, 40, and 41 have applied a thermodynamic method to determine the binding energy of EMs in Si crystals based on using the Saha relationship

$$n_{\mathrm{M}} = n_{\mathrm{ex}}^2 \left(\frac{4\pi\hbar^2}{M_{\mathrm{ex}}kT}\right)^{3/2} \frac{v_{\mathrm{M}}}{v_{\mathrm{ex}}^2} \exp\frac{\Delta_{\mathrm{M}}}{kT}. \tag{13}$$

The latter stems from the condition of equality of the chemi-

cal potentials of excitons and EMs (as calculated per e–h pair):

$$\mu_M = 2\mu_{ex}. \qquad (14)$$

Here $\nu_{M(ex)}$ is the multiplicity of degeneracy of the EM (or exciton) levels, and we have taken into account the fact that the translational mass of the molecule equals two exciton masses. As we noted above, this method must yield a reliable result if quasiequilibrium can be established between the components of the gas phase—excitons and EMs—within their lifetime. The measurements of the temperature dependence of the ratio I_M/I_{FE}^2 in Si ⟨100⟩ under conditions of bulk excitation in the temperature range 1.8–4 K performed in Ref. 29 yielded the value $\Delta_M = 0.6$ meV. Gourley and Wolfe[35,40] have realized conditions of a special inhomogeneous compression of Si crystals in which the gas of excitons and EMs proves to be located in a parabolic deformed potential well and does not contact the surface of the specimen. Under these conditions the lifetime τ_M of EMs was as much as $\sim 10^{-5}$ s, and the authors were able to measure the I_M/I_{FE}^2 variation in the temperature region 4.2–9 K. The value found for Δ_M proved to be 1.1 meV. The measurements of the binding energy of EMs in germanium performed in uniaxially compressed crystals[30,42] and based on measuring the variation of I_M/I_{FE}^2 in the temperature region 1.5–3 K (Fig. 5) yielded the value $\Delta_M = 0.27 \pm 0.06$ meV$\approx$0.1 Ry. In relation to the exciton Rydberg energy, this value is closer to that found in Si by Wolfe and Gourley.[40] It is not ruled out that equilibrium could not be established in the exciton system in the experiments with homogeneously compressed Si,[29] owing to the very small lifetime of EMs at $T < 4.2$ K ($\tau_M \sim 10^{-7}$ s). Hence the estimate of Δ_M proved to be too low.

In concluding this section we call attention to the fact that the experimental values of the binding energy of EMs in Si and in Ge ($\Delta_M \sim 0.10 \pm 0.02$ Ry) prove to be substantially larger than is expected, both from variational calculations, according to which $\Delta_M \approx 0.03$ Ry for $m_e \sim m_h$,[14] and from calculations based on the Monte-Carlo method and the Green's-function formalism ($\Delta_M \sim 0.06$ Ry).[17] It is not ruled out that deformational acoustic phonons make an appreciable contribution to increasing the stability of EMs in Si and Ge.

d) Impact dissociation of EMs by free carriers in a weak electric field

At high exciton densities in the gas phase, apprehensions arise that radiative recombination involving exciton-exciton collisions can contribute in the spectral region of emission of EMs (the M band). Within the framework of such a process, the intensity of emission is proportional to n_{ex}^2, while the width of the emission line is determined by the kinetic energy of the recoil exciton, just as in the case of emission from EMs. The contribution to the emission spectra from processes of inelastic exciton-exciton collisions can be distinguished by experiments on impact dissociation of weakly bound states by free carriers. When we take into account the fact that the binding energies of an EM and an exciton differ by more than an order of magnitude, in weak enough electric fields the carriers will mainly destroy the molecular states. Owing to the dissociation of EMs into free excitons, the EM radiation will disappear, whereas the rate of inelastic exciton-exciton collisions (and the corresponding emission channel in the spectra) will only increase under these conditions. The action of impact ionization on the emission spectra of EMs and excitons is illustrated in Fig. 6.[43] We see that the intensity of the M line in Si ⟨100⟩ at a mean density of e–h pairs $\sim 4\times10^{15}$ cm^{-3} declines appreciably even in fields $E = 10$ V/cm, while in fields $E = 50$–60 V/cm the M line completely disappears from the spectrum. Conversely, the free-exciton emission line in such small fields even increases somewhat owing to the displacement of

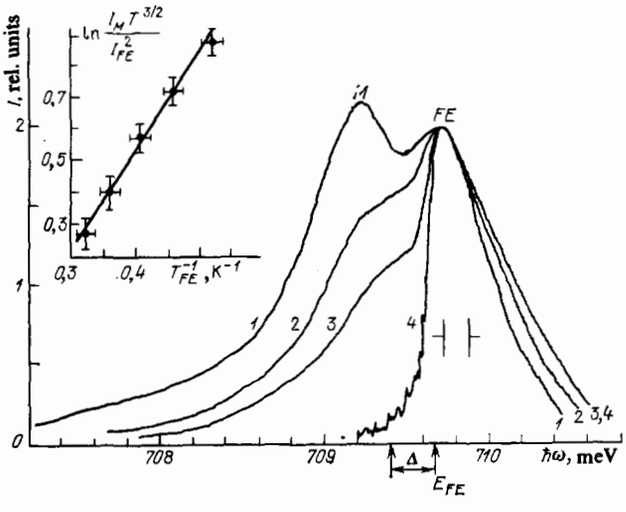

FIG. 5. Emission spectra of excitons and EMs inGe (~100).[30] 1–3: $W = 25$ W/cm^2; T_b (K) = 1.47 (1), 1.74 (2), and 2.1 (3); 4—$W = 3$ W/cm^2; $T_b = 2.1$ K. The inset shows the semilogarithmic dependence of ln $(I_M T_{ex}^{3/2}/I_{FE}^2)$ on T_{ex}^{-1}, from which the EM binding energy was determined.

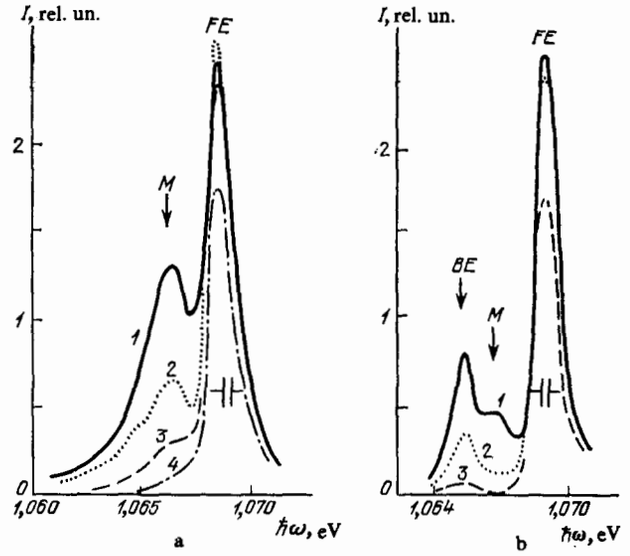

FIG. 6. Emission spectra of Si ⟨100⟩ at $T = 2$ K and excitation densities $\bar{n} \sim 4\times10^{15}$ cm^{-3} (a) and 3×10^{14} cm^{-3} (b).[43] Spectra 1–4 are recorded at an external field intensity of 0, 20, 40, and 60 V/cm, respectively.

the equilibrium between excitons and EMs in favor of excitons. An analogous result has also been obtained in studying EMs in Ge.[34] At low excitation densities, at which the emission line of bound excitons is also observed in the spectrum, applying an electric field primarily leads to disappearance of the EM line (Fig. 6). This result confirms the idea that the binding energy of an EM is substantially smaller than the binding energy of exciton-impurity complexes.

Thus the studies under conditions of impact dissociation allow one to rule out processes of exciton-exciton collisions and confirm that the M line arises from recombination of very weakly bound exciton states. We note also that the behavior of the M line in a weak electric field also contradicts the interpretation of this line in terms of radiative recombination of an ionized e–h plasma of low density. Actually, in this case in a weak electric field, the intensity of the M line could only increase owing to ionization of the excitons.

e) EMs in semiconductors with different numbers of electron valleys

In uniaxially compressed crystals of Ge $\langle\sim 100\rangle$, neither the electron nor hole bands are degenerate. Therefore both of the electrons (or holes) in an EM belong to the same electron (hole) extremum. In Si $\langle 100\rangle$, the conduction band contains two valleys x and $\bar{x}$ that lie on the compression axis $\langle 100\rangle$. Hence two electrons in an EM in Si $\langle 100\rangle$ can belong either to one valley (xx states), or to different valleys, but lying on one axis ($x\bar{x}$ states).

After the detection and identification of the EM emission lines in strongly compressed crystals of Si $\langle 100\rangle$, a very weak line was revealed[44] in very pure undeformed crystals of Si at $T = 1.4$ K (Fig. 7). Kaminskiĭ and Pokrovskiĭ[45] have also discovered an M line near the emission line of "hot" excitons in relatively weakly compressed crystals of Si $\langle 100\rangle$, and have attributed this line to emission from "hot" EMs that include one "cold" and one "hot" exciton.[2)] Emission lines of EMs have also been found[46] in Si crystals compressed along the $\langle 110\rangle$ axis. In contrast to "cold" EMs in Si $\langle 100\rangle$, both xx and $x\bar{x}$ states and xy states (with electrons

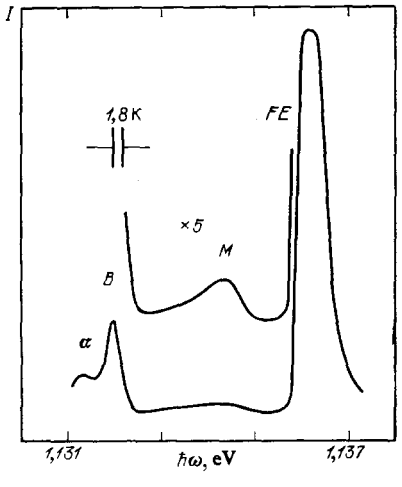

FIG. 7. The TA component of the emission spectrum of EMs and excitons in undeformed Si at 1.8 K.[44] α- and B emission of exciton-impurity complexes for phosphorus and boron, respectively.

from valleys whose principal axes are mutually perpendicular) are possible for electrons in EMs in undeformed Si and in Si $\langle 100\rangle$. In "hot" EMs in Si $\langle 100\rangle$ and Si $\langle 110\rangle$, the electronic states are only of the xy type. Due to the weakening of the Coulomb repulsion for xy electronic states (owing to the anisotropy of the electronic ellipsoids), one might expect that the binding energy of EMs with electronic states of the xy type will prove somewhat larger than with states of the xx (or $x\bar{x}$) type, just as for the D^- centers in Ge.[47] Reference 46 has studied the variation in the ratio of intensities of the emission lines of "hot" EMs and "hot" excitons, and "cold" EMs and "cold" excitons, as well as "hot" and "cold" EMs in Si $\langle 100\rangle$, with variation over a broad range of both the total exciton density and the relationship between the densities of "hot" and "cold" excitons. In agreement with the molecular nature of the M_h line, its intensity proved to be proportional to the product of the intensities of the emission lines of "cold" and "hot" excitons. A thermodynamic method was used to compare the binding energies of "hot" and "cold" EMs having xy and xx (or $x\bar{x}$) electronic states. Since the "cold" and "hot" excitions in EM lie in the same volume, we can start with the conditions of equality of chemical potentials (quasiequilibrium situation):

$$\mu_M^h = \mu_{ex}^c + \mu_{ex}^h, \qquad \mu_M^c = 2\mu_{ex}^c, \tag{15}$$

Then, when $n_M^H \ll n_M^c$, one can write[46]

$$\frac{I_M^h}{I_{FE}^h}\left(\frac{I_M^c}{I_{FE}^c}\right)^{-1} = \frac{1}{2}\left(\frac{M_M^h}{M_M^c}\right)^{3/2}\frac{\nu_M^h}{\nu_M^c}\frac{\nu_{ex}^c}{\nu_{ex}^h}\exp\frac{\Delta_M^h - \Delta_M^c}{kT}. \tag{16}$$

Here the superscripts h pertain to hot, and c to cold excitons (or EMs). The coefficient 1/2 appears because the annihilation of only one (hot) exciton in the EM contributes to the M_h line. In Si $\langle 100\rangle$ with two ground-state and four split-off valleys, we have $\nu_{ex}^c = 8$, $\nu_{ex}^h = 16$, $\nu_M^c = 6$, and $\nu_M^h = 32$. It has been found experimentally[46] that the binding energy Δ_M^h proved to be somewhat smaller than Δ_M^c: $\Delta_M^c = \Delta_M^h + 0.15$ meV, contrary to expectation. Yet, as was expected, the absolute change in the value of Δ_M proved to be small.

f) Multiexcitonic molecules

Exchange repulsion impedes the formation of EMs with a number of bound excitons greater than two in semiconductors with simple bands. In multivalley semiconductors having a valence band that is fourfold degenerate with respect to spin (like Ge and Si), this hindrance is lacking, owing to the large degeneracy of the bands. Wang and Kittel[50] have found that EMs are stable in the limiting case as $m_e/m_h \to 0$ with a number of excitons smaller than the multiplicity of degeneracy of the conduction band. Here the binding energy increases with increasing number of bound excitons. The reason for the strong binding is the relatively small contribution from the kinetic energy of the electrons, owing to the absence of nodes in the electronic wave function. In Si and Ge one can expect the existence of four-exciton molecules, since the smallest multiplicity of degeneracy of the (valence) bands is four. Such molecules must include excitons with "light" and

"heavy" masses. This raises the problem of their stability with respect to decay into two EMs made of excitons with "heavy" masses. The situation is more favorable in Si, where the corresponding splitting of the exciton term is small (~ 0.02 Ry[24]). Such multiexcitonic molecules have not yet been discovered. Experimental detection of them from radiative-recombination spectra is an extremely complex problem when one takes into account the extremely small partial fraction of such free multiexcitonic complexes in the exciton gas.

4. EXCITONIC MOLECULES IN A MAGNETIC FIELD (Si AND Ge)

a) Brief introduction

Let us examine the properties of EMs in a magnetic field. Owing to the extremely small scales of the binding energy, from the experimental standpoint an EM in uniaxially deformed crystals of Si and Ge proves to be a convenient model for studying the magnetic properties. Thus, for example, the limiting strong magnetic field at which the energies of paramagnetic splitting of the corresponding spin states of an electron (or hole) and the diamagnetic shift in the exciton begin to exceed the dissociation energy of the EM is attained in the easily realized fields $H \sim 8$ T for Si and $H \sim 1$ T for Ge. For the hydrogen molecule this situation arises in magnetic fields on an astronomical scale ($H > 10^6$ T).

The question arises of the stability of EMs when such magnetic fields are attained. Two cases are of interest in this regard that differ in the relationships between the lifetimes τ_{ex} and the spin relaxation times τ_s. When $\tau_s \gg \tau_{ex}$, there is no equilibrium between excitons in different spin states. Therefore, despite the formation of the molecules from two excitons existing in different spin states, the paramagnetic splitting in this case does not affect the stability of the EM in a magnetic field. The stability of the EM will decline with increasing magnetic field only when the diamagnetic contribution δE_M^d to its energy is more than twice the exciton contribution (δE_{ex}^d). The relationship $\tau_{ex} \ll \tau_s$ is realized in uniaxially deformed Si crystals.[51]

In the opposite case ($\tau_{ex} \gg \tau_s$), the excitons are distributed in an equilibrium manner among the spin sublevels, and the dissociation energy of the EM is sensitive to the paramagnetic splitting and declines with increasing magnetic field. This situation is observed in uniaxially deformed crystals of Ge.[30] The studies of EMs in uniaxially deformed crystals of Si and Ge in a magnetic field, which have successfully supplemented one another, allow one to distinguish unequivocally the diamagnetic and paramagnetic contributions. This problem is of definite interest, since one can draw two opposite conclusions a priori on the magnitude of the diamagnetic susceptibility of an EM, analogous to a positronium molecule. On the one hand, we can allow for the fact that $a_M \sim 3a_{ex}$,[13] by analogy with atoms, for which the diamagnetic susceptibility according to Langevin is proportional to the square of the distance of the electrons from the nucleus. Then we might expect the diamagnetic susceptibility χ_M of an EM to be an order of magnitude larger than that of an exciton: $\chi_M \sim 10\chi_{ex}$. On the other hand, the small biding energy of an EM indicates that the pair e–h correlations in an EM are apparently the same as in an exciton. Therefore χ_M can differ little from twice the value for an exciton.

b) Indirect excitons in a magnetic field

In the radiative decay reaction of a biexciton, the exciton state proves to be finite. Hence one can decide on the properties of EMs in a magnetic field by analyzing the relative position and spectral shifts of the corresponding Zeeman components in the emission spectra of excitons and EMs, their polarization and relative intensities. In this regard, we shall first take up the spectroscopic properties of indirect excitons in a magnetic field using the example of uniaxially deformed crystals of Si and Ge.[3)] In a magnetic field the ground state of an exciton in these crystals splits up into four spin sublevels. In small magnetic fields in which the cyclotron energy $\hbar\omega_c = eH/mc \ll$ Ry, one can write the energy of the split exciton terms in the form

$$E_{ex}(H) = E_{ex}(0) + (s_z g_e + j_z g_h)\,\mu_0 H + \frac{1}{2}\chi_{ex} H^2. \qquad (17)$$

Here s_z (j_z) is the projection of the spin of the electron (or hole), $g_{e(h)}$ are the g-factors of the electron (or hole), and μ_0 is the Bohr magneton. The selection rules for indirect transitions in Si and Ge have been derived in Refs. 53. They are given in Table I.

1) g-factors

We see from Eq. (17) that the magnitudes of the g-factors of an electron and a hole bound in an indirect exciton can be determined experimentally from the splitting of the corresponding Zeeman components in the spectra of indirect radiative annihilation of excitons. This can be done most simply in uniaxially compressed crystals of Si, in whose emission spectra one observes all four Zeeman components ($s_z, j_z = \pm 1/2$).[51] As one should expect, the g-factor of an electron in an exciton proved to be isotropic and close to two, while the g-factor of a hole is substantially anisotropic.[54] In the case of interest to us of uniaxially compressed Si for the geometry $\mathbf{H} \| \mathbf{P} \| \langle 001 \rangle$, we have $g_{h\|} = 1.1$[51] (Table II).

The large intensity of the Zeeman components of the emission spectrum corresponding to transitions from excited spin states of excitons under conditions in which the magnitude of the paramagnetic splitting amounts to several times kT indicates the absence of thermal equilibrium in the distribution of indirect excitons in uniaxially compressed silicon over the spin sublevels. This means that the spin relaxation times in uniaxially compressed silicon are substantially larger than their lifetimes τ_{ex} ($\tau_{ex} \approx 10^{-6}$ s).[29] We note that undeformed Si shows $\tau_s \approx 10^{-8} \ll \tau_{ex}$.[55] The great increase in the spin relaxation time in uniaxial compression of silicon is also observed in the exciton-impurity complexes.[56] In undeformed crystals the spin of a hole in the ground state (Γ_8) relaxes rapidly owing to spin-orbital mixing, while the spin relaxation time of an electron with an isotropic g-factor is determined by the electron-hole exchange interaction.[56] In uniaxially compressed crystals, the spin relaxation time of

TABLE I. Selection rules for indirect transitions in Si and Ge.

j_z, s_z:	3/2, −1/2	−3/2, 1/2	1/2, 1/2	−1/2, −1/2	1/2, −1/2	−1/2, 1/2
a Si, $\Gamma_8^+ - \Delta_6$						
Phonons						
LA	$-\gamma e_+ u_{LA}$	$-\gamma e_- u_{LA}$	$\frac{1}{\sqrt{3}}\gamma e_+ u_{LA}$	$\frac{1}{\sqrt{3}}\gamma e_- u_{LA}$	0	0
LO	$-\eta e_- u_{LO}$	$\eta e_+ u_{LO}$	$\frac{1}{\sqrt{3}}\eta e_- u_{LO}$	$-\frac{1}{\sqrt{3}}\eta e_+ u_{LO}$	$\sqrt{\frac{2}{3}}\lambda e_z u_{LO}$	$-\sqrt{\frac{2}{3}}\lambda e_z u_{LO}$
TO, TA	$-\alpha e_z u_-$	$\alpha e_z u_+$	$\frac{1}{\sqrt{3}}\alpha e_z u_-$	$-\frac{1}{\sqrt{3}}\alpha e_z u_+$	$-\sqrt{\frac{2}{3}}\beta(e_+ u_- + e_- u_+)$	$\sqrt{\frac{2}{3}}\beta(e_+ u_- + e_- u_+)$
b Ge, $\Gamma_8^+ - L_6$						
Phonons						
LA	$-\eta e_- u_{LA}$	$\eta e_+ u_{LA}$	$\frac{1}{\sqrt{3}}\eta e_- u_{LA}$	$-\frac{1}{\sqrt{3}}\eta e_+ u_{LA}$	$\sqrt{\frac{2}{3}}\lambda e_z u_{LA}$	$-\sqrt{\frac{2}{3}}\lambda e_z u_{LA}$
TO	$-(\alpha e_z u_- + \gamma e_+ u_+)$	$(\alpha e_z u_+ - \gamma e_- u_-)$	$\frac{1}{\sqrt{3}}(\alpha e_z u_- + \gamma e_+ u_+)$	$-\frac{1}{\sqrt{3}}(\alpha e_z u_+ + \gamma e_- u_-)$	$-\sqrt{\frac{2}{3}}\beta(e_+ u_- + e_- u_+)$	$\sqrt{\frac{2}{3}}\beta(e_+ u_- + e_- u_+)$

Here the z axis lies along the principal axis of the corresponding extremum. For Ge the x axis is chosen in one of the σ_v planes. In Si the direction of the x and y axes is arbitrary. The quantities j_z and s_z indicate the projections of the angular momenta of the holes ($j_z = \pm 3/2, \pm 1/2$) and of the electrons ($s_z = \pm 1/2$). The quantities u_i denote the amplitude of the displacements; α, β, γ, and η are constants; e is the polarization vector, and we have $e_\pm = e_x \pm ie_y$.

holes sharply increases owing to removal of degeneracy in the valence band.[57] In turn, the increase in τ_s for holes leads to increase in τ_s for electrons. As we shall show below, it is very important in understanding the problem of EMs in Si ⟨100⟩ in a magnetic field to take into account the long spin relaxation times, which lead to thermodynamic nonequilibrium between electrons in different spin states.

In Ge crystals the intensity of emission from excited spin states decreases rapidly with increasing spin splitting, and one cannot resolve the individual Zeeman components in the exciton emission spectra. Hence, in Ge the spin relaxation time proves to be substantially smaller than the lifetime of excitons, which amounts to $\sim 10^{-6}$ s, just as in Si. Such a strong difference in the magnitudes of τ_s in Si and Ge crystals involves the fact that in Ge, the contrast to Si, the electron g-factor is strongly anisotropic and momentum scattering leads to spin scattering.

The magnitudes of the g-factors of the electron and hole in an exciton in strongly compressed Ge with $\mathbf{H}\|\mathbf{P}\|$ ⟨100⟩ ($\mathbf{P} \approx 400$ MPa) have been determined[30] by analyzing the spectral distribution of the emission from indirect excitons in π^- and σ-polarizations in magnetic fields $H = 1$–4 T. With $\mathbf{H}\|\mathbf{P}\|$ ⟨100⟩, the g-factor for the electron ($g_e \approx 1.6$) proved to be close to that of a free electron ($g_e = 1.57$[58]), while the g-factor of the hole is $g_h = -4.5 \pm 1$, which is substantially larger than the g-factor of the hole in an exciton in undeformed Ge ($g_h = -1.6$[53]) and somewhat less than the g-factor of a free hole in extremely compressed Ge ($g_h = -6.8$[59]). Complete information on the electron and hole g-factors in an indirect exciton in uniaxially deformed

TABLE II. The g factors of electrons and holes in excitons and the diamagnetic susceptibilities of excitons and EMs in uniaxially compressed crystals Si ⟨100⟩, Ge ⟨111⟩, and Ge ⟨~100⟩. For comparison the g factors are also given of free electrons (g_e^*) and holes ($g_{h\|}^*$).

	Si ⟨100⟩	Ge ⟨~100⟩	Ge ⟨111⟩
g_e, experiment	1,9±0,1 [51]	1,6±0,1 [30]	1,0±0,2 [30]
g_e^*, »	2,0 [54]	1,57 [59]	0,9 [59]
$g_{h\|}$, »	1,2±0,2 [51]	4,5±1,0 [30]	4,5±1,0 [30]
$g_{h\|}^*$, »		6,8 [58]	6,8 [58]
meV/T:			
calculation	0,0045 [51]	0,18 [64]	0,27 [64]
experiment	0,004±0,0015 [51]	0,15±0,03 [30]	0,25±0,05 [30]
meV/T^2, experiment	0,010±0,002 [51]	0,50±0,08 [30]	—
χ_M/χ_{ex}:			
experiment	2,5±0,5 [51]	2,7±0,5 [30]	—
calculation	< 3,8 [72]	< 3,8 [72]	—

crystals of Si and Ge is found in Table II.

2) Diamagnetic susceptibility of indirect excitons in Si and Ge

One can determine the magnitude of the diamagnetic shift of the exciton term experimentally by analyzing the deviation of the $E_{ex}(H)$ relationship from linear. For this purpose it is convenient to represent the dependence of the shift of the exciton line in the spectrum on the magnitude of the magnetic field $\delta E_{FE} \equiv E_{FE}(s_z, j_z, H) - E_{FE}(H=0)$ in the coordinates $\delta E_{FE}/H$ and H. In the region of weak magnetic fields the variation of $\delta E_{FE}/H$ is approximated by a straight line whose slope yields the diamagnetic susceptibility, while the intersection with the axis of ordinates yields the magnitude of the overall g-factor of the electron and hole in the exciton. Figure 8 shows the experimental $\delta E_{FE} \cdot H^{-1}(H)$ relationships measured from the spectral shifts of the free-exciton emission line in Ge ($\sim$001) and Ge ⟨111⟩.[30] We see that a deviation of the relationship from linear sets in at rather strong magnetic fields $H \sim 1.5$ T, at which $\hbar\omega_c \sim$ Ry/2. Just as one should expect, the magnitude of χ_{ex} proves to be substantially anisotropic, owing to the strong anisotropy of the effective masses of electrons and holes. An analogous situation is observed also in Si.[51] The found values of χ_{ex} for different directions of the magnetic field and the uniaxial compression in Si and Ge are given in Table II.

In the region of small magnetic fields, one can calculate the diamagnetic susceptibility of indirect excitons with sufficient accuracy within the framework of perturbation theory

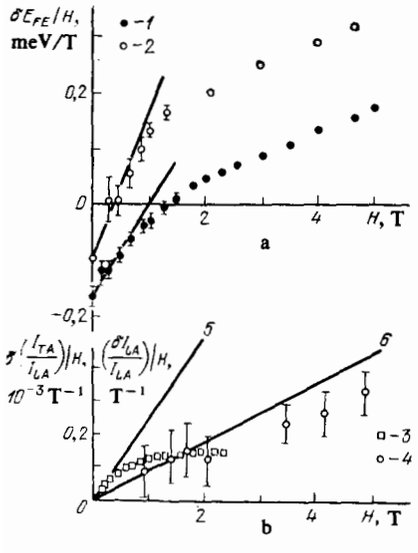

FIG. 8. Shift of the emission line of free excitons (a) and the variation of its intensity (b) in strongly uniaxially compressed Ge crystals as a function of the magnetic field. a—Symbols–experiment under the conditions $\mathbf{H}\|\mathbf{P}\|$ ⟨1.1.16⟩ (*1*) and $\mathbf{H}\|\mathbf{P}\|$ ⟨111⟩ (*2*),[30] solid lines—results of calculation[64]; b—$\mathbf{H}\|\mathbf{P}\|$ ⟨1.1.16⟩, symbols—experimental measurements of the integral intensity of the FE line in the allowed (LA) component: $(\delta I_{LA}/I_{LA})/H$ (*3*) and of the variation of the ratio of intensities of the forbidden (TA) and allowed (LA) components of the FE line: $\delta(I_{LA}/I_{LA})/H$ (*4*); the calculated dependences are shown respectively by the straight lines *5* and *6*.[69,68] To pick out the terms quadratic in the magnetic field, the measured quantity divided by the magnitude of the magnetic field is plotted as the ordinate.

if one takes into account the anisotropy of the spectrum of masses of electrons and holes. As is well known, the Hamiltonian of an electron with an isotropic spectrum moving in a central field (without taking spin motion into account) contains a correction to the energy of the ground state of the form $(e^2/8mc^2)\,[\mathbf{H}\times\mathbf{r}]^2$ (the so-called Langevin term).[60] If the effective masses of electrons and holes prove to be tensors, then the Hamiltonian describing the relative motion of the electron and the hole in an exciton with zero momentum of the center of gravity has the form[61]

$$\mathscr{H}^0 = \mathscr{H}_0 + \mathscr{H}_1 + \mathscr{H}_2. \tag{18}$$

Here we have

$$\mathscr{H}_0 = \frac{1}{2}\,\mathbf{p}m_{ex}^{-1}\mathbf{p} - \frac{e^2}{\varepsilon r}, \tag{19}$$

$$\mathscr{H}_1 = \frac{e}{c}\,[\mathbf{A}^e(\mathbf{r})\,m_e^{-1} - \mathbf{A}^h(\mathbf{r})\,m_h^{-1}]\,\mathbf{p}, \tag{20}$$

$$\mathscr{H}_2 = \frac{e^2}{2c^2}\,[\mathbf{A}^e(\mathbf{r})\,m_e^{-1}\mathbf{A}^e(\mathbf{r}) + \mathbf{A}^h(\mathbf{r})\,m_h^{-1}\mathbf{A}^h(\mathbf{r})] + \frac{3e^2}{c^2}\,\mathbf{A}(\mathbf{r})\,M_{ex}^{-1}\mathbf{A}(\mathbf{r}), \tag{21}$$

$$\mathbf{A}^{e,h}(\mathbf{r}) = \frac{1}{2}\,[\mathbf{H}m_{ex}m_{e,h}^{-1}\mathbf{r}], \quad \mathbf{A} = \mathbf{A}^e + \mathbf{A}^h,$$
$$m_{ex}^{-1} = m_e^{-1} + m_h^{-1}, \quad M_{ex} = m_e + m_h.$$

We assume that the products of coordinates and momenta in $\mathscr{H}_1$ have been symmetrized. We see from these expressions that a correction to the energy that is quadratic in the magnetic field arises not only for $\mathscr{H}_2$ in first-order perturbation theory (Langevin diamagnetism), but also from $\mathscr{H}_1$ in second-order theory (Van Vleck orbital paramagnetism). In the case of isotropic masses $\mathscr{H}_1$ goes over into[62,63]

$$\frac{e\hbar}{2m_{ex}c}\,\frac{m_h - m_e}{m_h + m_e}\,\mathbf{HL}. \tag{22}$$

The angular momentum of relative motion $\mathbf{L}$ is conserved. In the ground state we have $\mathbf{L} = 0$. Hence orbital paramagnetism dos not exist in the isotropic limit.

Calculations of χ_{ex} for excitons in uniaxially compressed Ge have been performed in Ref. 64. In such crystals having a nondegenerate valence band, the spin motion is separated with good accuracy from the orbital motion, which is described by the Hamiltonian of (18). Despite the large anisotropy of the effective masses, it turned out that the fundamental contribution χ_{ex} stems from the Langevin term. In particular, both in Ge ⟨100⟩ and in Ge ⟨111⟩ the Van Vleck correction does not exceed several percent and can be neglected. The authors of Ref. 64 obtained the following expression for the diamagnetic-susceptibility tensor for indirect excitons in Ge in the crystal system of coordinates (i.e., $x\|\langle 100\rangle$, $y\|\langle 010\rangle$, and $z\|\langle 001\rangle$):

$$\chi_{ik} = -\begin{vmatrix} 0{,}26 & 0{,}05 & 0{,}06 \\ 0{,}05 & 0{,}26 & 0{,}06 \\ 0{,}06 & 0{,}06 & 0{,}18 \end{vmatrix}\ \text{MeV/T}^2. \tag{23}$$

This tensor determines the diamagnetic correction to the energy, which is given by the formula

$$\delta E_{ex}^{d} = -\frac{1}{2}\,\chi_{ik}H_iH_k, \quad i,\ k = 1,\ 2,\ 3. \tag{24}$$

For the electron valleys lying along the ⟨111⟩, ⟨$\bar{1}$11⟩, ⟨1$\bar{1}$1⟩,

and $\langle 11\bar{1}\rangle$ axes, the field **H** is respectively equal to

$$(H_x,\ H_y,\ H_z),\quad (H_y,\ -H_x,\ H_z),\quad (H_y,\ H_x,\ H_z)$$

and $(-H_x,\ -H_y,\ H_z)$.

All the components H_i are defined with respect to the crystallographic axes.

Upon compressing Ge along the $\langle 111\rangle$ direction, the diamagnetic susceptibility tensor contains two components $\chi_{ex\parallel}$ and $\chi_{ex\perp}$, which are longitudinal and transverse with respect to H. They are equal to

$$\chi_{ex\perp} = -0.46\ \text{MeV/T}^2,\quad \chi_{ex\parallel} = -0.52\ \text{MeV/T}^2\ [64].$$

The calculated and experimental values of the diamagnetic susceptibilities are compared in Fig. 8 and Table II. We see that they agree well among themselves. A comparison of the diamagnetic susceptibilities of excitons in Ge and Si and in hydrogen atoms, for which $\chi_H = 8.1\times 10^{-17}$ MeV/T^2, shows that χ_{ex} (Si) is 8 orders of magnitude, and χ_{ex} (Ge) 10 orders of magnitude larger than χ_H.

3) Magneto-Stark effect of indirect excitons

In the translational motion of a free exciton in a transverse magnetic field in the system of coordinates associated with the center of mass of the exciton, the electric field $\vec{\mathscr{E}} = (p/M_{ex}c)\times\mathbf{H}$ arises (M_{ex} and **p** are the translational mass and the momentum of the exciton). The appearance of an electric field is due to the fact that the Lorentz term $(2e/M_{ex}c)\mathbf{p}\cdot\mathbf{A}(\mathbf{r})$ appears in the two-particle Hamiltonian of (18). In combination with $\mathscr{H}^0$ and $P^2/2M_{ex}$, it determines the complete perturbation operator. This electric field polarizes the exciton and leads to mixing of p-type antisymmetric states into its ground state. Owing to this mixing, the resultant wave function of the free exciton loses the property of symmetry with respect to inversion of coordinates. This phenomenon, which has been named the magneto-Stark effect, has been employed to study the internal structure and properties of translational symmetry of direct excitons using the example of CdS crystals.[65–67]

Here we shall treat one of the interesting manifestations of the magneto-Stark effect in indirect exciton annihilation spectra in uniaxially deformed Ge crystals.[68] Exciton-phonon transitions in Ge can be either allowed (with participation of odd TO- and LA-phonons), for which the transition matrix element $g_{al}(\mathbf{k}_e\mathbf{k}_h)\neq 0$ when $\mathbf{k}_e = \mathbf{k}_h = 0$, or forbidden (with participation of even TA- and LO-phonons), for which $g_f = 0$ when $\mathbf{k}_e = \mathbf{k}_h = 0$.[37] In a first approximation we have $g_{al} = g_0$, $g_f = \eta_e\cdot\mathbf{k}_e + \eta_h\cdot\mathbf{k}_h$. The amplitudes of indirect annihilation of an exciton with the momentum **p**, accompanied by emission of a phonon with the momentum **q** with respect to the minimum of the electron valley, are respectively equal for allowed and forbidden transitions in the isotropic case to:

$$A_{al} = g_0\delta(\mathbf{p}-\mathbf{q})\,\psi^{\mathbf{p}}_{ex}(0), \tag{25}$$

$$A_f = \delta(\mathbf{p}-\mathbf{q})\,[\mathbf{b}\mathbf{p}\psi^{\mathbf{p}}_{ex}(0) - ic\nabla\psi^{\mathbf{p}}_{ex}(0)]. \tag{26}$$

Here we have $b = (\eta_e m_e + \eta_h m_h)M_{ex}^{-1}$, and $c = \eta_e - \eta_h$. In the absence of a magnetic field, the wave function of the ground state of the exciton is centrosymmetric, even when the spectrum of effective masses is anisotropic. Hence we have $\nabla\psi^{\mathbf{p}}_{ex}(0) = 0$, and the contribution of both the allowed and forbidden components is determined only by the quantity $\psi^{\mathbf{p}}_{ex}(0)$. First of all, applying the magnetic field causes a transverse compression of the wave function of the ground state of the exciton $\psi^0_{ex}(\mathbf{r})$[69]:

$$\psi^0_{ex}(\mathbf{r}) = \frac{\exp(-r/a_{ex})}{\pi^{1/2}} \times\left\{1 + \left(\frac{\hbar\omega_c}{4R}\right)^2\left[\frac{11}{6} - \frac{r}{6a_{ex}}\left(1+\frac{3}{2}\sin^2\theta\right) - \frac{r^3}{6a_{ex}^3}\sin^3\theta\right]\right\} \tag{27}$$

(Here θ is the angle between **r** and **H**). This leads to the same increase in the amplitudes of indirect exciton annihilation, both for allowed and forbidden transitions. The situation changes radically for excitons moving across the magnetic field, for which another term is added to the intrinsic wave function $\psi^0_{ex}(r)$ of the operator $\mathscr{H}^0$, owing to the Lorentz term in the Hamiltonian polarizing the exciton[4]:

$$\psi^{\mathbf{p}}_{ex}(\mathbf{r}) = \psi^0_{ex}(r) - \psi^0_{ex}(r)\frac{\varepsilon a_{ex}}{e}\vec{\mathscr{E}}r\left(1+\frac{r}{2a_{ex}}\right). \tag{28}$$

Here the wave function of the exciton loses the property of central symmetry, since $\nabla\psi^{\mathbf{p}}_{ex}(r)$ differs from zero and equals

$$\nabla\psi^{\mathbf{p}}_{ex}(0) = -\psi^0_{ex}(0)\frac{\varepsilon a_{ex}}{e}\vec{\mathscr{E}}. \tag{29}$$

Here the following correction to the kinetic energy arises:

$$-\frac{9}{4}\varepsilon a_{ex}^3\mathscr{E}^2 = \frac{p_\perp^2}{2M_{ex}}\frac{9m_{ex}}{8M_{ex}}\left(\frac{\hbar\omega_c}{R}\right)^2. \tag{30}$$

This implies an increase in the magnetic field of the translational mass of the exciton in the direction perpendicular to **H**.

One can derive the following expression from Eqs. (25), (26), (28), and (29) for the ratio of intensities of the forbidden and allowed components of the exciton-phonon luminescence[68]:

$$\frac{I_f}{I_{al}}(H) = \left\langle \mathbf{b}\cdot\mathbf{p} + \mathbf{c}\ \frac{\vec{\varepsilon}\mathscr{E}a_{ex}}{e}\right\rangle. \tag{31}$$

Here the angle brackets denote averaging over the Boltzmann distribution of the excitons. A dependence on the magnetic field arises twice in Eq. (31): first, since $\mathscr{E}\sim H$, and second, owing to the redistribution of excitons in momentum space because of the change in translational mass. Thus the more rapid increase in the intensity of the forbidden component as compared with the allowed component arises exclusively from the magneto-Stark effect.

Figure 8 compares the experimental and theoretical variations of the ratio of intensities of the forbidden and allowed components I_f/I_{al} for excitons in Ge $\langle\sim 100\rangle$. The calculation employed the values $m_{ex}/M_{ex} = 1/8$, $a_{ex} = 160$ Å,[64] and the ratio of parameters $|c|/|b| = 2$, which stems from the ratio $\eta_e^2/\eta_h^2 \leqslant 1/10$. The weak-field approximation $\hbar\omega_c \ll$ Ry within which the calculation was performed is valid in fields $H < 0.7$–1 T. It was found[69] that the $I_{al}(H)$ relationship begins specifically in these fields to differ from quadratic. We see from Fig. 8 that the ratio I_f/I_{al}, where the

factor $\psi_{ex}^0(0)$ has been cancelled, is well described over a broader range of fields (up to $H \sim 3$ T).

We should stress the difference between the magnetic properties of atomic gases and excitons in semiconductors. The corrections to the wave function of an exciton at rest, which are proportional to H^2, are determined by the reduced mass, and hence are analogous to the corresponding corrections in atoms. But the corrections for the magnetic-Stark effect are determined by the translational mass M. Consequently they are more substantial for excitons, since $M_{at} \gg M_{ex}$.

c) Diamagnetic susceptibility of EMs

We should expect by analogy with the hydrogen molecule that EMs in the ground state in strongly compressed Ge crystals having simple electron and hole bands will have a zero resultant spin moment. In this case one can write the energy of the EM in the region of weak magnetic fields in the form

$$E_M(H) = E_M(0) + \frac{1}{2}\chi_M H^2. \quad (32)$$

Taking into account expression (17) for the energy of the exciton term, we find that the change in binding energy of the EM in the magnetic field for $s_z, j_z = \pm 1/2$ is

$$\Delta_M(H) - \Delta_M(0) = (|g_e| + |g_h|)\mu_0 H + \frac{1}{2}\delta\chi \cdot H^2. \quad (33)$$

Here we have $\delta\chi = 2\chi_{ex} - \chi_M$.

A somewhat different situation exists in Si uniaxially deformed along the ⟨001⟩ axis, where the electrons in the ground state of the EM can exist in different valleys and have a total spin $S = 1$. For these EMs the binding energy does not depend at all on the splitting associated with the electron spin. Moreover, as we have noted above, in strongly compressed Si crystals thermal equilibrium is lacking between the different paramagnetically split exciton terms. Therefore, from the thermodynamic standpoint excitons in different spin states are independent components, while the change in effective binding energy of EMs is determined only by the difference of the diamagnetic susceptibilities χ_M and $2\chi_{ex}$:

$$\Delta_M(H) - \Delta_M(0) = \frac{1}{2}\delta\chi \cdot H^2. \quad (34)$$

By using Eqs. (32)–(34) and the values indicated above for χ_{ex}, $g_{e,h}$, and $\Delta_M(0)$, one can estimate the magnitude of the critical field in which EMs must break down. When $\chi_M = 10\chi_{ex}$, EMs would have to break down only because of their large diamagnetism: in Si at $H = 1$ T, and in Ge as low as $H \sim 0.2$ T. When $\chi_M = 2\chi_{ex}$, EMs in Si should remain stable in any fields, while EMs in Ge would break down owing to spin splitting of electrons and holes at $H \sim 1.5$ T.

Édel'shteĭn[72] has calculated the diamagnetic susceptibility of excitonic molecules. He examined the corrections to the energy proportional to the square of the magnetic field that arise both in first-order (Langevin diamagnetism) and in second-order perturbation theory (Van Vleck orbital paramagnetism). In particular, it was established that for a biexciton the Langevin correction to the energy does not reduce to the mean of the square of any distance, as occurs in a multielectron atom. The calculations employed the variational EM wave function taken from Ref. 14. The magnitudes of the Langevin and Van Vleck corrections depend on the choice of the system of coordinates, whereas their sum is constant. The least value of the Langevin correction to the energy found[72] by numerical integration proved to be

$$\delta E_M^d \approx 11{,}4\frac{e^2H^2}{6m_{ex}c^2}a_{ex}^2. \quad (35)$$

We recall that for a single exciton the diamagnetic energy shift is

$$\delta E_{ex}^d \approx 3\frac{e^2H^2}{6m_{ex}c^2}a_{ex}^2. \quad (36)$$

Hence, while taking account of the fact that the Van Vleck paramagnetic term yields a negative contribution to the energy of the ground state of the EM, we have the following estimate[72] for the ratio of diamagnetic susceptibilities of a biexciton and an exciton:

$$\frac{\chi_M}{2\chi_{ex}} < 1{,}9, \quad (37)$$

According to this, χ_M differs slightly from twice the susceptibility of a free exciton.

Experimental studies of the effect of a magnetic field on the stability of EMs have been performed for Si[41,51] and for Ge.[30,42] EMs in Si remain stable throughout the studied field interval $H < 8$ T. The EM emission line broadens in a magnetic field owing to the Zeeman splitting of the final state—the exciton. The change in binding energy of EMs in Si in a magnetic field has been estimated[41] from the change in the ratio of intensities of the emission lines of EMs and excitons at fixed temperature. When H is increased to 8T at 2 K, I_M/I_{FE} diminishes by a factor less than three. This implies that $\chi_M < 2.7\chi_{ex}$.

In germanium, in contrast to silicon, the intensity of the EM emission line in a magnetic field rapidly declines, and this line practically disappears in the spectrum at fields as low as $H \sim 1.5$ T, even at $T = 1.6$ K (Fig. 9). Here the FE

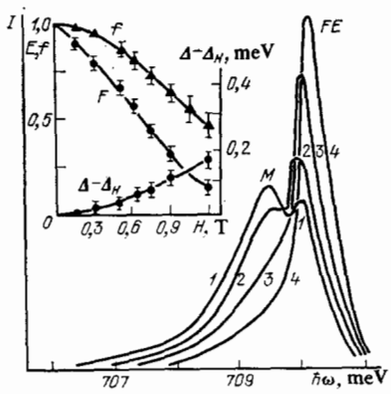

FIG. 9. Effect of a magnetic field on the emission spectra of excitons and EMs in Ge (~001).[30] Spectra 1–4 are recorded at $T_b = 1.5$ K. $H = 0$, 0.4, 0.8, and 1.2 T, respectively. The inset shows the variation in a magnetic field of the ratio of intensities of the emission lines of EMs and excitons I_M/I_{FE}^2. Experiment—curve F: calculation without taking into account the diamagnetic shifts of the FE and M lines (i.e., with $\delta E_M = 2\delta E_{ex}$—curve f. The variation of the binding energy of an EM obtained from the ratio of the experimental values of F and f is the curve $\Delta - \Delta_H$.

line increases, owing to the increased number of excitons arising from dissociation of EMs. The integral emission intensity varies weakly, since the quantum yields of EMs and excitons are similar. The experimentally found value of the critical magnetic field for EMs is close to that estimated above, starting only from the values of the spin splitting of electrons and holes. Hence χ_M is close to $2\chi_{ex}$ also in Ge. The magnitude of χ_M was determined by analyzing the dependence on the magnetic field of the ratio of intensities of the exciton and EM lines.[30] Under conditions of thermodynamic equilibrium, the equality of the chemical potentials $H_M = 2\mu_{ex}$ implies that in the gas phase the variation of the ratio n_M/n_{ex}^2 in a magnetic field must be described by the relationship[30]

$$F(H) \equiv \frac{n_M(H)}{n_{ex}^2(H)} \left(\frac{n_M(0)}{n_{ex}^2(0)}\right)^{-1} = \exp\left(\frac{H^2\delta\chi/2}{kT}\right) f(g_e, g_h, H, T). \quad (38)$$

Here the densities of excitons and EMs at $H = 0$ are related by Eq. (13). The function f describes the decrease in the fraction of EMs owing to paramagnetic splitting:

$$f = 4\left[\cosh\frac{(g_e+g_h)\mu_0 H}{2kT} + \cosh\frac{(g_e-g_h)\mu_0 H}{kT}\right]^{-2}. \quad (39)$$

The experimental variation of I_M/I_{FE}^2 (see the inset of Fig. 9) implies that in Ge, just as in Si, we have $\chi_M = (2.5 \pm 0.5)\chi_{ex}$.

Interestingly, in a fixed magnetic field such that the spin splitting $(|g_e| + |g_h|)\mu_0 H$ is larger than the binding energy $\Delta_M(0)$ of EMs, the relative fraction of EMs in Ge does not decrease. Conversely, it increases with increasing temperature, owing to the redistribution of excitons over the spin sublevels and the filling of the excited spin states. Such an increase in the fraction of EMs is observed experimentally in crystals of Ge $\langle\sim 100\rangle$ at $H = 1$–1.2 T in the temperature range 1.5–2.5 K.

Thus the studies of EMs in Ge $\langle\sim 100\rangle$ and Si $\langle 100\rangle$ in a magnetic field imply that, despite the large dimensions of EMs, their diamagnetic susceptibility is close to twice the value for an exciton. This result agrees with the measurements of χ_M in the direct-band semiconductor CdS[73] that showed that $\chi_M = 2.4\chi_{ex}$. Hence the pairwise electron-hole correlations in an EM are just as strong as in a free exciton. The destabilization of EMs in germanium mainly involves the fact that excitons having spin-oriented electrons and holes cannot form a stable molecular state owing to the strong exchange repulsion. We call attention to the fact that above we have only treated the limit of rather weak magnetic fields $\hbar\omega_c < \mathrm{Ry}$, in which the excitons are not yet diamagnetic.

Spin-oriented exciton gas in uniaxially deformed Ge

A well known theoretical concept based on the integer values of the exciton spin predicts the quantum statistical behavior of a high density system of excitons in semiconductors at low temperatures and the possibility of Bose-Einstein condensation of excitons if the repulsion among excitons at close distances predominates over the van der Waals attraction.[74–77] As we discussed above, attractive forces predominate among ordinary excitons in semiconductors, and they are bound into EMs or into a dense metallic electron-hole liquid. A qualitatively different situation arises in experiments with excitons in strongly uniaxially compressed Ge $\langle\sim 001\rangle$ crystals. In this case at $T \lesssim 2$ K, and $H > 1$ T, where the paramagnetic splitting in the exciton becomes larger than $\Delta_M(0)$ and the mean thermal energy of the excitons, EMs turn out to become dissociated owing to the exchange repulsion between the spin-oriented excitons. It was also found experimentally that magnetic fields up to 5 T do not stabilize the electron-hole liquid (owing to the large magnitude of the diamagnetic contribution to the energy of the ground state of the liquid phase involving Landau diamagnetism[33]). Therefore a unique opportunity arises in Ge $\langle\sim 001\rangle$ in magnetic fields $H = 2$–5 T at low temperatures of studying the quantum-statistical behavior of a spin-oriented exciton gas up to densities at which their ionization breakdown sets in[78,79]

One can extract information on the statistical behavior of an exciton gas upon changing its density by analyzing the form of the exciton-phonon emission spectra. The corresponding experiment has been performed in Refs. 78 and 79 (Fig. 10). With increasing exciton concentration, the exciton line first narrows in accord with the change in the distribution of excitons in the band according to the Bose-Einstein statistics:

$$I_{FE}(E) \sim \sqrt{E} f_{BE} = \sqrt{E}\left[\exp\left(\frac{E-\mu_{ex}}{kT}\right) - 1\right]^{-1}. \quad (40)$$

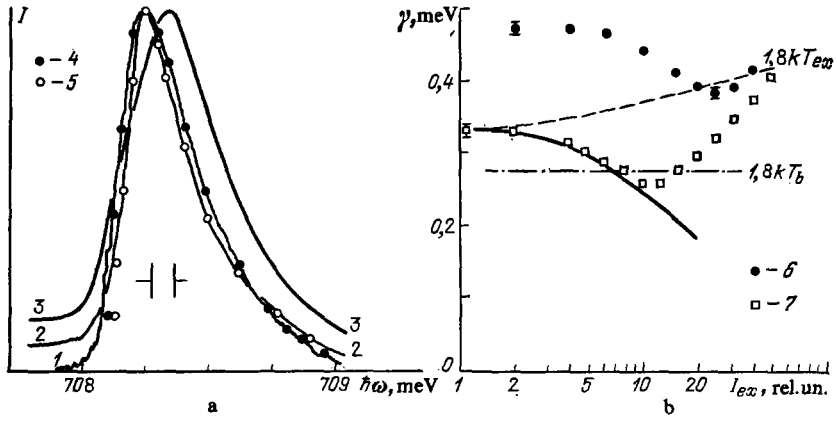

FIG. 10. Variation of the LA component of the emission spectrum (π-polarization) of spin-oriented excitons in Ge $\langle\sim 100\rangle$ with increasing excitation density.[78,79] a—$H = 5$ T, $T_b = 1.75$ K, W (W/cm^2) = 3 (1), 40 (2), and 200 (3). The symbols show the approximation of the shape of the spectrum within the framework of the Boltzmann (4) and Bose-Einstein distribution of excitons (5): experiment at $T_b = 1.75$ K (7) and 2.15 K (6). The expected $\gamma(T_{ex})$ dependence for an ideal Bose gas of excitons is shown by the solid line, by the dot-dash line for a Boltzmann distribution of excitons (without taking into account the heating of the exciton system), and by the dotted line taking this heating into account).

At large n_{ex} the interaction between excitons begins to take effect and the exciton emission line begins to broaden (see Fig. 10). Under conditions in which the interaction between excitons is small, one can independently determine their chemical potential μ_{ex} in these experiments by approximating the shape of the exciton emission line by Eq. (40). Hence one can determine the density of excitons. Up to concentrations of excitons corresponding to the dimensionless parameter $r_s = 3$, the exciton gas still remains weakly interactive. (The parameter r_s characterizes the density of excitons in units of the Bohr radius $r_s = [(3/4\pi)na_{ex}^3]^{1/3}$.) We see from Fig. 10 that the interaction beween the excitons primarily broadens the red edge of the exciton emission line and shifts its maximum toward the violet. The effective scattering length of excitons was first estimated experimentally from this broadening, and proved to be $a_s^{ex} \approx a_{ex}$. This value of a_s is close to that known for hydrogen $a_s^H \sim 0.8a_H$,[80] and is substantially smaller than that expected from the calculations: $a_s^{ex} \sim 8a_{ex}$.[81,82] In the case of a spin-oriented exciton gas in Ge $\langle \sim 001 \rangle$, it has not yet been possible to realize conditions corresponding to Bose-Einstein condensation. As is known, for an ideal Bose gas the critical concentration for condensation in momentum space is connected to the temperature by the relationship[83]

$$n_c = \frac{\nu (MT)^{3/2}}{(3,31)^{3/2}\hbar^2}. \qquad (41)$$

Here ν is the multiplicity of degeneracy, and M is the mass. Equation (41) implies that the critical density is $r_s^c \approx 3.2\, T^{-1/2}$ (K) for a spin-oriented exciton gas in Ge. In the region of experimentally realizable temperatures $T \gtrsim 2$ K, r_s^c proves to be less than 2.3. That is, it lies in a range of densities where the excitons break down owing to screening of the Coulomb interaction in such a dense exciton system.[79,84–86] Further decrease in the temperature involves considerable experimental difficulties because of the nonequilibrium nature of the exciton system. Nevertheless it is evident that a spin-oriented exciton gas with the example of Ge $\langle \sim 001 \rangle$ is a new, nontrivial quantum object.

We note also that studies of the form of the emission line of a very dense exciton gas have been recently conducted in the direct-band semiconductor Cu_2O having dipole-forbidden direct transitions.[87,88] In these crystals the formation of EMs is impossible owing to the strong exchange interaction.[89] Consequently one can obtain large densities of excitons in Cu_2O. No narrowing of the emission lines with increasing excitation density was observed[87,88] for either the singlet or triplet excitons. However, it was found, first, that the increase in the half-width of the triplet exciton line with increasing W occurs more slowly than was expected from the estimates of the heating of the exciton system by the exciting radiation, and second, that a very broad long-wavelength edge appears in this line at large W. These results agree well with those obtained for indirect excitons in Ge $\langle \sim 100 \rangle$.

d) EMs in a strong magnetic field

Up to now we have been treating the effect on EMs of weak magnetic fields in which the magnetic energy is a weak perturbation as compared with the Coulomb energy, i.e., under conditions with $\hbar\omega_c < \text{Ry}$. Under these conditions the lower state is a singlet term with $\mathbf{S} = \mathbf{J} = 0$, while the triplet term ($\mathbf{S}$ and/or $\mathbf{J} = 1$) is repulsive. Here $\mathbf{S}$ characterizes the total spin of the electrons, and $\mathbf{J}$ that of the holes. For hydrogen the repulsive character of the triplet term is conserved at distances $R \simeq 8a_H$, where a_H is the Bohr radius of the hydrogen atom.[60] The magnetic field splits this term, and for large fields ($\hbar\omega_c \gg \text{Ry}$) it can turn out that not only does its lower branch fall below the singlet term, but also the depth of the potential well for this branch will suffice for formation of a bound state.[90–93]

The dissociation of EMs in a magnetic field $H \sim 1$–5 T found in germanium involves the fact that in these fields spin-oriented electrons and holes can still not form stable molecular orbitals with triplet states of the electrons and holes. The region of fields $H \leqslant 8$ T experimentally studied up to now in both Si and Ge is still far from the limit of strong magnetic fields treated in Refs. 90–93 in which one expects stabilization of molecular states. Realization of this limit for germanium requires fields of the order of several tens of teslas.

5. EXCITONIC MOLECULES IN DIRECT-BAND SEMICONDUCTORS

Now we shall examine the optical phenomena involving excitonic molecules in direct-band semiconductors. In these semiconductors the resonance excitation and radiative decay of biexcitons can occur without participation of phonons. The probabilities of direct transitions allowed in the zero order in the wave vector and accompanied by creation of or emission from biexcitons exceed by many orders of magnitude the corresponding probabilities for indirect-band semiconductors. The lifetimes of biexcitons for direct phononless recombination are so short that generally thermodynamic equilibrium is not established in the system of excitons and biexcitons. Hence nonlinear-optical methods have been developed for the experimental study of the properties of biexcitons in these semiconductors—two-photon excitation, two-photon Raman scattering, etc.—which have proved to be most effective under such nonequilibrium conditions. The methods of nonlinear optics are less suitable for studying biexciton spectra in indirect-band semiconductors, owing to the low probability of the corresponding transitions.

Further, as is known, direct dipole-allowed transitions to exciton states occur with strong light-exciton mixing.[94] Hence, at low enough temperatures and under conditions close to resonance two-photon excitation or scattering involving biexcitons, polariton effects become substantial. These effects are lacking in indirect recombination with participation of Brillouin phonons.

We shall examine the fundamental properties of biexcitons and the methods of studying them on the example of cadmium sulfide, a direct-band semiconductor with the wurtzite structure (symmetry group C_{6v}) where the extrema of the conduction band and the highest valence band have the symmetries Γ_7 and Γ_9 respectively, and lie in the

center of the Brillouin zone. If we neglect the anisotropy of the crystal, the dependences of the energies E_{ex} of excitons and E_M of biexcitons on their wave vectors $\mathbf{k}_x$ and $\mathbf{K}$ are described by the relationships

$$E_{ex}(\mathbf{k}_x) = E_{ex}(0) + \frac{\hbar^2 \mathbf{k}_x^2}{2M_{ex}},$$

$$E_M(\mathbf{K}) = E_M(0) + \frac{\hbar^2 \mathbf{K}^2}{2M}.$$

Here $M_{ex} = m_e + m_h$ and $M = 2M_{ex}$ are the translational masses of an exciton and a biexciton, respectively. In CdS $m_e \approx 0.2\, m_0$ is isotropic, while m_h is anisotropic. The principal values of the mass tensor for holes are $m_{h\perp} \approx 0.7\, m_0$ and $m_{h\parallel} \approx 5\, m_0$. The binding energy Δ_M of EMs in CdS is defined as $\Delta_M = 2E^t_{ex}(0) - E_M(0)$, where $E^t_{ex}(0)$ is the energy of the lowest state of a triple exciton.

a) Light-induced conversion of an exciton into a biexciton

One can write the Hamiltonian of excitons and EMs interaction with light in the second-quantization representation in the form[95]

$$H = H_{ex} + H_M + H_p + H_{exp} + H_{pM}.$$

Here we have

$$H_{ex} = \sum_{\mathbf{k}_x} E_{ex}(\mathbf{k}_x)\, b^+_{\mathbf{k}_x} b_{\mathbf{k}_x}, \qquad H_M = \sum_{\mathbf{K}} E_M(\mathbf{K})\, C^+_{\mathbf{K}} C_{\mathbf{K}},$$

$$H_p = \sum_{\mathbf{q}} \hbar\omega(\mathbf{q})\, a^+_{\mathbf{q}} a_{\mathbf{q}},$$

while H_{ex}, and H_M and H_p are the Hamiltonians of noninteracting excitons, EMs, and photons, and $b^+_{\mathbf{k}_x}$, $b_{\mathbf{k}_x}$, $C^+_{\mathbf{K}}$, $C_{\mathbf{K}}$, and $a^+_{\mathbf{q}}$, $a_{\mathbf{q}}$ are their corresponding creation and annihilation operators. The process of one-photon absorption with creation of an exciton is defined by the Hamiltonian

$$H_{exp} = \sum_{\mathbf{k}} g b_{\mathbf{k}} (a^+_{\mathbf{k}} + a_{-\mathbf{k}}) + \text{c.c.}$$

Here g is the exciton-photon coupling constant, while the oscillator strength of the dipole-allowed transition to the ground state f_{ex} is proportional to the square of the radial component of the exciton wave function at zero $|\psi_{ex}(0)|^2$.[38]

The Hamiltonian H_{pM} describes the process in which we are interested of absorption of a photon of energy $\hbar\omega(\mathbf{q})$ in the presence of an exciton of energy $E_{ex}(\mathbf{k}_x)$ to form a biexciton of energy $E_M = E_{ex} + \hbar\omega$ and momentum $\hbar\mathbf{K} = \hbar\mathbf{k}_x + \hbar\mathbf{q} \simeq \hbar\mathbf{k}_x$ ($\mathbf{q} = 2\pi/\lambda$ is the wave number of the photon):

$$H_{pM} = \sum G_M(\mathbf{K})\, C^+_{\mathbf{K}} (b_{\mathbf{k}_x} + b^+_{-\mathbf{k}_x}) \times (a_{\mathbf{q}} + a^+_{-\mathbf{q}})\, \delta(\mathbf{K} - \mathbf{k}_x - \mathbf{q}) + \text{c.c.}$$

Here $G_M(\mathbf{K})$ is the coupling constant with the field of photons. The probability of this process can be written in the form[95]

$$P_1(\mathbf{K};\ \mathbf{k}_x,\ \mathbf{q}) = \frac{2\pi}{\hbar} |\langle \mathbf{K}| H_{pM} |\mathbf{k}_x,\ \mathbf{q}\rangle|^2\, \delta(E_M - E_{ex} - \hbar\omega)$$

$$= \frac{2\pi}{\hbar} |G_M(\mathbf{K})|^2\, \delta(\mathbf{K} - \mathbf{k}_x - \mathbf{q}) \times \delta\left[E_{ex}(0) - \Delta_M + \frac{\hbar^2 \mathbf{K}^2}{4M_{ex}} - \hbar\omega\right]. \qquad (42)$$

Here $G_M(\mathbf{K})$ is determined by the wave function of the biexciton, which generally can be rather complicated.[13,14] To estimate the oscillator strength in the simplest approximation in which $\Delta_M \ll$ Ry, the biexciton can be treated as a structure consisting of two weakly bound excitons. Then the wave functions of the excitons are weakly deformed upon combining into a biexciton, and one can represent the wave function of the EM in the form of the symmetrized product of the wave function of the excitons ψ_{ex} and the function $F(R_h)$ that describes the relative motion of the excitons in the biexciton.[9,96] In this case the matrix element $G_M(\mathbf{K})$ will be proportional to the Fourier transform of the wave function $F(R_h)$, while the oscillator strength of the transition as recalculated per exciton is determined by the expression

$$f_M(K) = f_M(0) \left[1 + \left(\frac{a_M K^2}{2}\right)^2\right]^{-2}.$$

Here $a_M = \sqrt{\hbar^2/M\Delta_M}$ is a quantity of the order of the dimensions of the biexciton, while we have

$$\frac{f_M(0)}{f_{ex}} = \frac{16\pi a_M^3}{\Omega} \gg 1. \qquad (43)$$

Here Ω is the volume of the unit cell of the crystal.

Equation (43), which was first derived by Rashba *et al.*,[9,97] shows that the process of light-induced conversion of an exciton into an EM in direct-band semiconductors is characterized by gigantic oscillator strengths.

Upon multiplying (42) by the distribution function of the excitons in the band and summing over all $\mathbf{k}_x$, one can calculate the shape of the induced-absorption line, as has been done in a number of studies.[96,98,99]

In the experimental study of induced conversion of excitons into biexcitons, the specimen is usually excited with laser radiation in the region of interband transitions. Thereby a certain distribution of excitons is formed in the exciton band, which can be described in the quasiequilibrium case by a Boltzman distribution with the temperature T_{ex}. A weak broad-band probe radiation is passed through the volume of the specimen to be excited, and its transmission spectrum is recorded as a function of the density or distribution of the excitons. Here one observes rather broad bands of one-photon absorption that indicate the formation of biexcitons. The induced conversion of excitons into a biexciton is also manifested in other experiments,[100] e.g., involving four-wave mixing near a two-photon biexciton resonance (see below).

However, satisfactory theoretical approximations of the experimentally observed induced-absorption bands are yet lacking. The point is that one must know the distribution of the excitons in the band in calculating the induced absorption. In the case of CdS other difficulties also arise that involve the anisotropy of its band spectrum, and the dependence of the energy of the excitons and biexcitons, not only on the absolute magnitude, but also on the direction of their wave vectors. Moreover, the binding energy of a biexciton is comparable with the magnitude of the longitudinal-transverse splitting Δ_{LT}. Therefore one must allow for polariton effects in calculating biexciton absorption.

b) Giant two-photon absorption creating a biexciton

A very simple nonlinear optical effect manifesting an anomalously large transition oscillator strength is two-photon absorption.[8] The process of two-photon absorption as treated in second-order perturbation occurs via an intermediate exciton state for which the matrix element g of the transition is proportional to $\psi_{ex}(0)$. The second stage of the process consists in combination of a second exciton with the virtual exciton, and is characterized by the matrix element $G_M(K)$. The absorption of two photons of energy $\hbar\omega(\mathbf{q})$ forms a biexciton with energy $E_M = 2\hbar\omega$ and wave vector $\mathbf{K} = 2\mathbf{q}$. The resulting transition probability has the form[95]

$$P_2(\mathbf{K};\ \mathbf{q}) = \frac{2\pi}{\hbar}\left|\sum_{\mathbf{k}_x}\frac{\langle \mathbf{K}\,|H_{pM}|\,\mathbf{k}_x,\ \mathbf{q}\rangle\langle \mathbf{k}_x,\ \mathbf{q}\,|H_{exp}|\,\mathbf{q},\ \mathbf{q}\rangle}{E_{ex}(\mathbf{k}_x)-\hbar\omega(\mathbf{q})}\right|^2 \times\delta(E_M(\mathbf{K})-2\hbar\omega(\mathbf{q})) = \frac{2\pi}{\hbar}\left|\frac{G_M(0)\,g}{\Delta_M}\right|^2\delta(\mathbf{K}-2\mathbf{q})\,\delta(E_M-2\hbar\omega). \quad (44)$$

One can easily compare the probability of two-photon absorption with the probability P_{ex} of one-photon exciton absorption within the framework of the model of weakly bound excitons in the biexciton. In this approximation it is not complicated to show[97] that their ratio is

$$\frac{P_2}{P_{ex}} \sim \left(\frac{\mathrm{Ry}}{\Delta_M}\right)^{3/2}\left(\frac{E_0}{\Delta_M}\right)^2.$$

Here E_0 is a quantity of the order of the width of the exciton band. Here the left-hand factor has been derived by integrating the numerator of (44), and is of the order of 10^2–10^3. The right-hand factor, which is of the order of 10^4, arose from the resonance denominator in (44). Thus the resulting probability of the studied two-photon absorption is anomalously large, so that the process has been called "giant two-photon absorption." The intensity of this absorption is proportional to the density of photons. According to Ref. 8, it can even be comparable with that of one-photon exciton absorption under reasonable excitation conditions (e.g., at 10^7 W·cm^{-2} for CuCl).

Resonance excitation of biexcitons in the process of giant two-photon absorption has been detected in the cubic crystals CuCl and CuBr in the transmission spectra[101] and in the excitation spectra of the biexciton radiative-recombination spectra M_L.[102] It was not possible for a long time to detect manifestations of giant two-photon absorption in CdS.[103,104] The experimental difficulties that arose partly involved the fact that the two-photon absorption lines in CdS were masked by intense absorption bands of exciton-impurity complexes (EICs) observed in the transmission and excitation spectra of the specimens under study.[105,106] Hence the reliable studies of giant two-photon absorption have been performed with specially purified specimens of CdS having a content of shallow impurities less than 10^{15} cm^{-1}, in which the exciton-impurity-complex lines were weaker than the two-photon absorption lines.[107,108]

Let us present examples of transmission spectra of CdS with laser excitation. Figure 11 shows the spectral dependence of laser radiation transmitted through a CdS specimen in the polarization $\mathbf{E}\perp\mathbf{C}$, $\mathbf{q}\perp\mathbf{C}$. The curves 1–5 correspond to

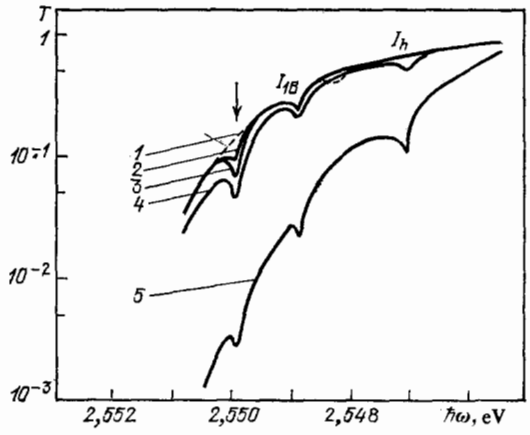

FIG. 11. Spectral dependence of the intensity of monochromatic laser radiation transmitted through CdS and polarized with $\mathbf{E}\perp\mathbf{C}$ at a temperature of 2 K.[107] Curves 1—5 correspond to pumping of 10, 10^2, 10^3, 10^4, and 10^5 W/cm^2.

power densities of the exciting radiation from 10 to 10^5 W/cm^2. As we see from the diagram, one distinctly observes narrow absorption lines with energies 2.5499 eV (486.102 nm); 2.5488 eV (486.312 nm); and 2.5470 eV (486.665 nm) on the background of the gently sloping tail of the exciton band, which shifts with increasing excitation level toward longer wavelengths. The latter two lines involve formation of EICs I_{1B} and I_h, and their intensity declines with increasing level of excitation owing to saturation of absorption. The line at 2.5499 eV, whose intensity increases more than linearly in the pumping range from 10^2 to 3×10^4 W/cm^2 and saturates at higher levels of excitation, involves resonance two-photon absorption to give rise to a biexciton. It is observed only upon probing the specimen with narrow-band laser radiation and is not manifested in the transmission spectra of the specimen at any power densities if the probe radiation is broad-band. Actually, when the specimen is probed with radiation having a small half-width γ_i of the laser line, absorption arises only at the frequency $\hbar\omega = E_M/2$, while the half-width of the absorption line is $2\gamma_i$.[109] When the specimen is probed with broad-band radiation, as will be shown below, biexcitons can be created with absorption of any two photons with energies $\hbar\omega_1$ and $\hbar\omega_2$ that satisfy the condition $\hbar\omega_1 + \hbar\omega_2 = E_M$. In this case one observes an increased absorption involving biexcitons in a rather broad spectral region below the exciton resonance instead of a sharply marked absorption line.[110,111]

Giant two-photon absorption is manifested in the excitation spectra of the M- and P-bands of biexciton emission,[110,111] in studying the modulation transmisssion spectra of CdS,[114] and in a number of other indirect experiments. By using giant two-photon absorption, one can rather accurately determine the binding energy Δ_M and the biexciton excitation energy $E_M(0)$. For CdS these quantities proved to be the following[107,108,112]: $\Delta_M = 4.4 \pm 0.2$ meV, $E_M = 5.0998$ eV at $T \lesssim 2$ K.

c) Polariton effects

The elementary approach to treating the phenomena of induced and two-photon absorpiton that we have employed

above has allowed proving the existence of the biexciton in direct-band semiconductors and determining their characteristic parameters. However,the quantitative agreement between the experimentally observed shape of the biexciton absorption and and the theoretical predictions has been unsatisfactory. The various steps taken to improve the theory, such as the introduction of the decays γ_{ex} and γ_M of the exciton and biexciton states, the allowance for longitudinal-transverse splitting of the exciton states, and their nonequilibrium occupancy, did not lead to appreciable progress in describing experiment.

The point is that the processes of induced and giant two-photon absorption to create a biexciton are distinguished by high probabilities only in the presence of strong exciton-photon interaction. Therefore, in the studied region of the spectrum one requires taking a more rigorous account of the mixing of exciton and photon states, i.e., going over to the polariton representation. Here one automatically takes account of the difference between longitudinal, transverse, and mixed exciton states and the effects of spatial dispersion and retardation.

Upon going over to the polariton representation, new single-particle states arise in the medium instead of transverse excitons and photons—excitonic polaritons, which correspond to bound exciton-photon states.[115-117] The energy of a polariton $\hbar\omega_p$ and its wave vector $\mathbf{k}$ are connected by a dispersion relationship of the following form[118-120]:

$$\epsilon_b + \frac{4\pi\beta(\hbar\omega)^2}{[E_{ex}(\mathbf{k}) - i\gamma_{ex}]^2 - (\hbar\omega)^2} = \frac{c^2k^2}{\omega^2}. \quad (45)$$

Here ϵ_b is the background dielectric permittivity, $4\pi\beta$ is the exciton polarizability, and γ_{ex} is the decay constant of the exciton.

In Fig. 12 the solid curves show the solutions of Eq. (45), which correspond to the lower and upper polariton branches. The dotted line shows the photon dispersion curve $\hbar\omega_T = \hbar kc/n$, while the dashed line is that of transverse excitons $E_{ex}^T(K_x^T)$. The dot-dash line shows the curve $E_{ex}^L(k_x^L)$, which is the solution of the equation $\epsilon = (k_x^L)^2c^2/\omega^2 = 0$, and which corresponds to longitudinal excitons, which do not interact with light. We see from the diagram that the dispersion curves of polaritons differ appreciably from the corresponding dispersion curves of photons and transverse excitons only near exciton resonance (i.e., with k close to that of light). Far from exciton resonance, where the dispersion curves of polaritons practically coincide with the dispersion curves of photons and excitons, one speaks respectively of "photon-like" and "exciton-like" polaritons. The contribution of the "photon" and "exciton" components to the polariton state is determined by the coefficients $A(k)$ and $B(k)$[96,121]:

$$A = (1-x^2)[1+4\pi\beta(1-x^2)]^{1/4}(\sqrt{(1-x^2)^2+4\pi\beta})^{-1},$$

$$B = \sqrt{4\pi\beta/[(1-x^2)^2+4\pi\beta]}.$$

Here we have $x = \hbar\omega(k)/E_{ex}^T(k)$.

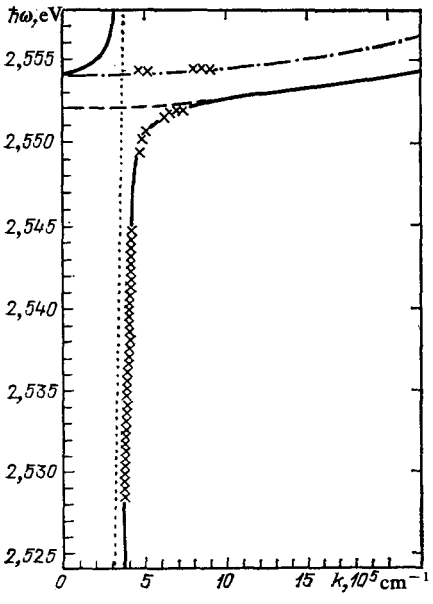

FIG. 12. Dispersion curves of excitons, photons, and polaritons near exciton resonance in CdS at liquid-helium temperature.[126] The crosses give the experimental values of $\hbar\omega_p(k)$ obtained by the HRS method.

In Refs. 20 and 122, the energy structure of biexciton states was determined and the selection rules for the process of two-photon absorption to form biexcitons in direct-band semiconductors were studied. In particular, for CdS the matrix element of the transition corresponding to absorption of two photons of energies $\hbar\omega_1$ and $\hbar\omega_2$ to form a biexciton in the ground state Γ_1 is proportional to $\mathbf{e}_{1\perp}\cdot\mathbf{e}_{2\perp}$—the scalar product of the projections of the polarization vectors $\mathbf{e}_1$ and $\mathbf{e}_2$ of the photons on a plane perpendicular to the C axis of the crystal.[123]

When we take this into account, the probability of formation of a biexciton by combination of two polaritons of energies $\hbar\omega_1$ and $\hbar\omega_2$, wave vectors $\mathbf{k}_1$ and $\mathbf{k}_2$, and polarizations $\mathbf{e}_1$ and $\mathbf{e}_2$ is described by the following relationship according to Ref. 95:

$$P(\mathbf{K};\ \mathbf{k}_1,\ \mathbf{k}_2) = \frac{2\pi}{\hbar}|(\mathbf{e}_{1\perp}\cdot\mathbf{e}_{2\perp})|^2 |G_M(\mathbf{K})[A(\mathbf{k}_1)B(\mathbf{k}_2) + A(\mathbf{k}_2)B(\mathbf{k}_1)]|^2 \delta(\mathbf{K}-\mathbf{k}_1-\mathbf{k}_2) \times \delta(E_M-\hbar\omega_1-\hbar\omega_2). \quad (46)$$

Here, as before, $G_M(\mathbf{K})$ denotes the matrix element of the transition. This process of absorption of two polaritons results in forming a biexciton with the energy $E_M = \hbar\omega_1 + \hbar\omega_2$ and wave vector $\mathbf{K} = \mathbf{k}_1 + \mathbf{k}_2$, in accord with the conservation laws. The probability of the process depends little on whether the polaritons are "exciton-like" or "photon-like," on how much their energies differ, or on whether they are formed by photons of laser radiation or have arisen from thermalization of excitons after interband excitation. Thus the transition to the polariton representation eliminates the distinction between "giant two-photon" and "induced" absorption: both processes are described in the language of absorption of two polaritons with the probability given by Eq. (46).

d) Reabsorption induced by biexcitons. Dispersion of biexcitons

Modified variants of induced absorption were employed in Ref. 124 to study biexciton states. The specimen

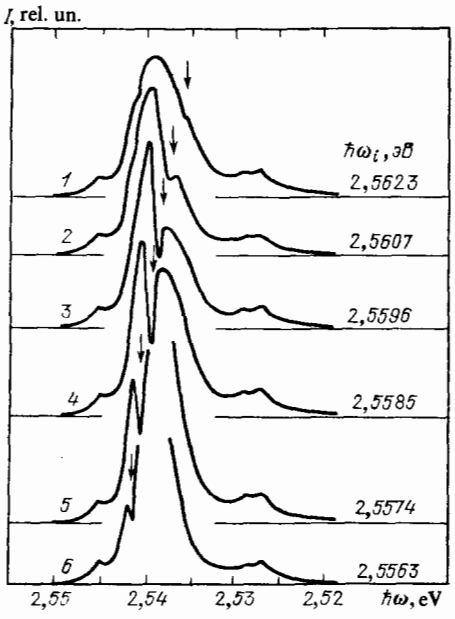

FIG. 13. Luminescence spectra of CdS in which reabsorption lines induced by biexcitons are observed at a temperature of 5 K and with different photon energies $\hbar\omega_i$ of the exciting radiation with power 10^5 W/cm^2.[125]

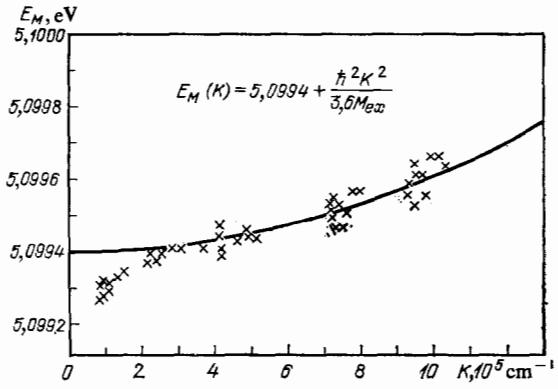

FIG. 14. Dispersion curve $E_M(K)$ of Γ_1 biexcitons in CdS at temperature 5 K as measured by the method of induced reabsorption.[126]

was excited with laser radiation with a photon energy $\hbar\omega_1 < E_{ex}(0)$. Thus a nonequilibrium distribution of polaritons was created with energies $\hbar\omega_1 + \gamma_1$. Further, as is usual, the excited volume of the specimen was probed with a weak broad-band radiation and its transmission spectrum was studied. Reference 125 proposed using the recombination radiation proper that arises from the excited volume as the probe light to record the biexciton absorption, and to study the spectrum of its reabsorption. In Fig. 13 curves 1–6 show the luminescence spectra of CdS at liquid-helium temperature as excited with tunable laser radiation with photon energies from 2.5623 to 2.5563 eV and an excitation power density of 10^5 W/cm^2. We see that the luminescence spectra distinctly show minima, whose position $\hbar\omega_{abs}$ shifts upon varying the energy of the exciting photons $\hbar\omega_i$ so that the sum $\hbar\omega_{abs} + \hbar\omega_i$ does not depend on $\hbar\omega_i$ and varies significantly upon varying the direction of the wave vectors of the photons of the exciting radiation $\mathbf{q}_i$.

The observed reabsorption involves the absorption of the photons of the recombination radiation having the energy $\hbar\omega_{abs}$ and wave vector $\mathbf{k}_{abs}$, which form biexcitons with energies $E_M = \hbar\omega_i + \hbar\omega_{abs}$ and wave vectors $\mathbf{K} = \mathbf{q}_i + \mathbf{k}_{abs}$ together with the polaritons generated by the laser. It is possible experimentally to vary from 0° to 180° the angle between the direction of the wave vector of the exciting photons $\mathbf{q}_i$ and the direction of observation of the recombination radiation from which the photons with wave vectors $\mathbf{k}_{abs}$ are absorbed. Then the wave vector of the biexcitons generated by the observed reabsorption will vary from $|\mathbf{K}^{max}| = |\mathbf{q}_i| + \mathbf{k}_{abs}| \approx 2q_i = 2\omega_i n/c \approx 10^6$ cm^{-1} to $|\mathbf{K}^{min}| \approx \mathbf{q}_i| - \mathbf{K}_{abs}| \approx 0$. Biexcitons with different wave vectors $\mathbf{K}^{min} < \mathbf{K} < \mathbf{K}^{max}$ have slightly differing values of the energy $E_M(K)$, as has been observed experimentally.[126] Figure 14 shows the experimental dependence of the biexciton energy $E_M = \hbar\omega_{abs} + \hbar\omega_i$ on the magnitude of the wave vectors of the biexciton $|\mathbf{K}| = |\mathbf{q}_i + \mathbf{k}_{abs}|$ measured at different angles between $\mathbf{q}_i$ and $\mathbf{k}_{abs}$. The solid line shows the curve $E_M(K) = E_M(0) + (\hbar^2K^2/2M)$ that gives the best agreement with the experimental results. The adjustable parameters found as a result, $E_M(0) = 5.0994$ eV and $M = (1.7–2.4)\,M_{ex}$ agree well with the data obtained by other methods.

We note that, when the angle between $\mathbf{q}_i$ and $\mathbf{k}_{abs}$ is varied, when both radiations are polarized perpendicularly to the **C** axis of the CdS crystal, the intensity of the reabsorption lines varies in accord with the factor $|\mathbf{e}_{i1}\cdot\mathbf{e}_{abs1}|^2$. An analogous variation is observed upon varying the angle beween the polarization vectors $\mathbf{e}_i$ and $\mathbf{e}_{abs}$ in the case in which the exciting and reabsorbed radiations propagate parallel to the **C** axis. These angle and polarization measurements have made possible unequivocal establishment of the fact that two-polariton absorption excites the totally symmetric state of the crystal Γ_1, which corresponds to two bound pairs of electrons and holes, i.e., a biexciton. The observed biexciton is free; that is, it can migrate through the crystal. Its translations mass is $M = (2.0 \pm 0.4)M_{ex}$, while the binding energy with respect to decay into two Γ_6 excitons is 4.4–4.8 meV.

As we see from Figs. 11 and 13, the intensities of the giant two-photon and induced absorption lines are comparable or exceed the intensity of the one-photon absorption lines with formation of EICs, which correspond to oscillator strengths of the order of unity. With increasing temperature, the half-width of the biexciton absorption lines increases, and they disappear from the transmission spectrum at 20–25 K. The latter involves process of thermal dissociation of biexcitons and their scattering by phonons.

e) Hyper-Raman scattering via an intermediate biexciton state

An important instrument for studying the structure and spectrum of biexcitons and polaritons in direct-band semiconductors is hyper-Raman (or two-photon Raman) scattering (HRS). As we showed above, if the energy of the exciting photons $\hbar\omega_i$ is $E_M/2$, then biexcitons are created in resonance. In times of the order of 10^{-9}–10^{-10} s they are thermalized and then recombine radiatively. If the sum of

the energy of the two photons of laser radiation does not correspond to the two-photon resonance of biexcitons, then in this case only virtual biexcitons are excited, which decay into two polaritons. We shall call the one of these polaritons with the energy E_f and momentum $\hbar\mathbf{k}_f$ the recoil polariton. It can be either "exciton-like" or "photon-like," depending on the conditions for observing HRS. The other photon-like polariton with the energy E_R and wave vector k_R escapes from the crystal in the direction of observation and is detected in the form of scattered radiation. In contrast to the case of strict resonance two-photon excitation, in the intermediate state here relaxation of biexcitons does not occur, while the HRS process itself obeys the following laws of conservation of energy and momentum:

$$2\hbar\omega_i = E_R + E_f, \quad 2\mathbf{k}_i = \mathbf{k}_R + \mathbf{k}_f. \tag{47}$$

Thus HRS is an inseparable process of two-photon absorption and radiative decay into two polaritons in which the conservation laws (47) are satisfied, and its probability in second-order perturbation theory is described by the expression[95]

$$P_{\text{HRS}} = \frac{2\pi}{\hbar}\frac{|C(2\mathbf{k}_i; 2\mathbf{k}_i-\mathbf{k}_R, \mathbf{k}_R)C(2\mathbf{k}_i; \mathbf{k}_i, \mathbf{k}_i)|^2}{E_M(2\mathbf{k}_i)-2\hbar\omega_i(\mathbf{k}_i)} \times \delta(E_f(\mathbf{k}_f)+E_R(\mathbf{k}_R)-2\hbar\omega_i(\mathbf{k}_i)). \tag{48}$$

The right-hand matrix element $C(2\mathbf{k}_i; \mathbf{k}_i, \mathbf{k}_i = 4|G_M \times (2\mathbf{k}_i)A(\mathbf{k}_i)B(\mathbf{k}_i)|^2$ corresponds to transition from the ground state of the crystal to an intermediate biexciton state upon absorbing two identical transverse Γ_5 polaritons. It is nonzero only for transitions to the totally symmetric Γ_1 state of the biexciton. The left-hand matrix element is

$$C(2\mathbf{k}_i; \mathbf{k}_f, \mathbf{k}_R) = |(\mathbf{e}_{f\perp}\mathbf{e}_{R\blacktriangle})G_M(2\mathbf{k}_i)[A(\mathbf{k}_f)B(\mathbf{k}_R)-A(\mathbf{k}_R)B(\mathbf{k}_f)]|^2.$$

This depends on the angle between the vectors $\mathbf{k}_R$ and $\mathbf{k}_f = 2\mathbf{k}_i - \mathbf{k}_R$ in accordance with the "geometric factor" $|\mathbf{e}_{f\perp}\cdot\mathbf{e}_{R\perp}|^2$, where $\mathbf{e}_{R\perp}$ and $\mathbf{e}_{f\perp}$ are the projections of the polarization vectors of the scattered polariton and the recoil polariton on a plane perpendicular to the hexagonal axis of the crystal.

We shall treat the case below in which all the polaritons participating in the HRS process have wave vectors lying in the plane $(\mathbf{k}_x, \mathbf{k}_y)$ perpendicular to the C axis of the CdS crystal. Depending on the direction of observation of the scattered radiation $\mathbf{n}_R = \mathbf{k}_R/|\mathbf{k}_R|$, we shall distinguish "back," "side," and "forward" scattering.

Figure 15 illustrates the HRS process. In the case of back scattering (Fig. 15a), two identical photons of the laser radiation excite a state of the crystal with the wave vector $2\mathbf{k}_i$ and the energy $\hbar\omega_i$ close to the biexciton Γ_1 state. This intermediate state decays into a photon-like polariton with the wave vector $\mathbf{k}_R^T$ directed opposite to $\mathbf{k}_i$ and an exciton-like transverse recoil polariton with the wave vector R_f^T of the order of magnitude of $3\mathbf{k}_i$ and with energy $E_f^T(k_f^T) \approx E_{ex}^T(0) + (\hbar^2 k_f^T)^2/2M_{ex}$. The intermediate state can decay also into a photon-like polariton with energy $\hbar\omega_R^L$ and a longitudinal exciton with energy

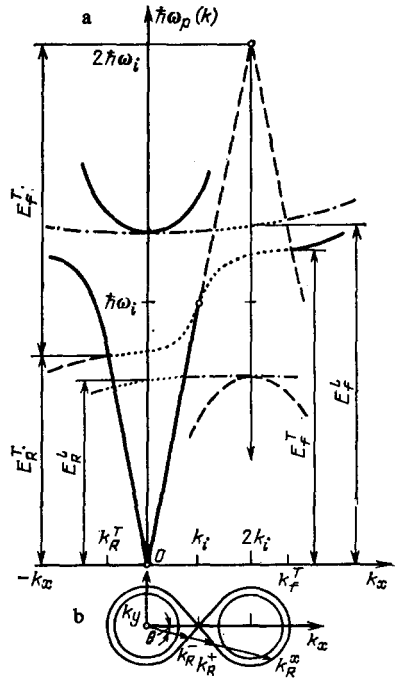

FIG. 15. Diagram of the HRS process upon excitation of the semiconductor with photons of energy $\hbar\omega_i$ and momentum $\hbar k_i$. The laws of conservation of energy and momentum (47) are satisfied in the space $(\hbar\omega, \mathbf{k}_x, \mathbf{k}_y)$ at the geometric locus of the points whose projection on the $(\hbar\omega, \mathbf{k}_x)$ plane is shown by the dotted line in Fig. 15a, and on the $(\mathbf{k}_x, \mathbf{k}_y)$ plane by the solid curves in Fig. 15b.

$E_f^L(k_f^L) = E_{ex}^L(0) + (\hbar^2 k_f^L)^2/2M_{ex}$ and wave vector $\mathbf{k}_f^L$ directed opposite to $\mathbf{k}_i$. In both cases the laws of conservation of energy and momentum (47) are obeyed, so that, as the energy of the photons $\hbar\omega_i$ of the exciting radiation is varied, the spectral position of the HRS line $\hbar\omega_R$ varies in accordance with the expressions

$$E_R^T = 2\hbar\omega_i - E_f^T(\mathbf{k}_f^T), \quad E_R^L = 2\hbar\omega_i - E_f^L(\mathbf{k}_f^L). \tag{49}$$

An HRS phenomenon involving biexciton states was first discovered in CuCl crystals.[11,127,128] in Refs. 107, 112, and 129, in addition to the known EIC luminescence lines, two intense HRS lines were observed in the emission spectra of CdS, which were called R_T and R_L. Their spectral positions $\hbar\omega_R^T$ and $\hbar\omega_R^L$ varied in accordance with the relationship (49),[130] while the relative intensities of the lines depended on the direction of observation. Owing to the "geometric factor" in back observation, the intensity of the R_L line was considerably weaker than that of the R_T line, while the R_L line dominated in side scattering.

The intensity of the lines in both cases increased, in accordance with (48), as $\hbar\omega_i$ approached $E_M/2$. This made possible an independent determination of the position of the biexciton level $E_M(K = 2k_i) = 5.0998$ eV, and establishment of its symmetry as Γ_1 from the angular and polarization dependences of the intensities of the HRS lines.[107,126,131]

The behavior of the HRS lines in forward scattering at small angles $\theta < 30°$ differs considerably from the case of back or side scattering. Figure 16 shows the HRS spectra in CdS crystals at the temperature 2 K, scattering angle $\theta = 15°$,

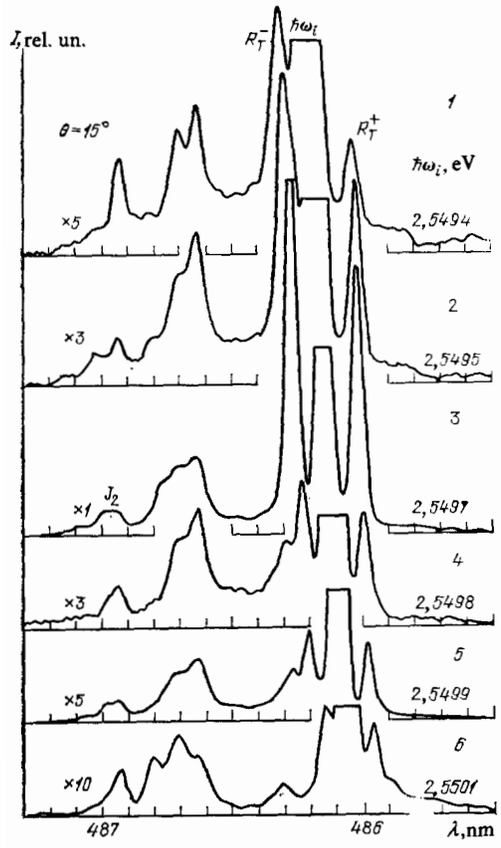

FIG. 16. HRS spectra in CdS in "forward" observation at an angle $\theta = 15°$ at temperature 2 K and with different photon energies of the laser radiation (curves 1–6, respectively).

power density of the exciting laser radiation 10^3 W/cm^2, and photon energy from 2.5494 to 2.5501 eV.

As we see from the diagram, in addition to the EIC lines, one observes two lines R_T^+ and R_T^- in the emission spectra that lie approximately symmetrically about the laser line $\hbar\omega_i$. The intensity of these lines increases in resonance fashion as $\hbar\omega_i$ approaches $E_M/2$. The variation of the wave vectors $\mathbf{k}_R^+$ and $\mathbf{k}_R^-$ associated with them with varying scattering angle is illustrated by Fig. 15b, which shows the projection of the geometric locus of the points satisfying the laws of conservation of energy and momentum (47) for a given $\hbar\omega_i$ in the form of a figure-eight. As we see from the diagram, polaritons with the wave vectors $\mathbf{k}_R^+$, $\mathbf{k}_R^-$, and $\mathbf{k}_R^x$ can be scattered in the direction of observation characterized by the angle θ while satisfying the conservation laws. A polariton with a larger wave vector $\mathbf{k}_R^x$ (of the order of $3\mathbf{k}_i$) is "exciton-like," and a weak HRS line corresponding to it is observed only in very thin perfect CdS specimens.

As the scattering angle decreases from $\theta_{max} \approx 30°$ to 0° for constant $\hbar\omega_i$, the absolute magnitude of the wave vector $\mathbf{k}_R^-$ increases, while $\mathbf{k}_R^+$ decreases while approaching $\mathbf{k}_i$. Hence the corresponding HRS lines in the emission spectra of CdS R_T^- and R_T^+ approach the line $\hbar\omega_i$ of the exciting laser radiation. Upon fixing the parameters ϵ_b, $E_{ex}^T(0)$, $4\pi\beta$, and M_{ex}, which determine the dispersion law for transverse polaritons (45), the dependence of the spectral position of the R_T^+, R_T^-, and R_T^x lines in CdS on the scattering angle θ has been calculated[95] for different values of $\hbar\omega_i$ of the exciting laser radiation. Figure 17 gives the experimental positions of the R_T^+ and R_T^- lines as a function of the photon energy $\hbar\omega_i$ for the three scattering angles 3°, 19°, and 45°. The solid lines show the corresponding results of the theoretical calculations obtained by solving the system of equations (47) under the condition that the polariton dispersion law is described by Eq. (45) with the generally adopted parameters ϵ_b, $E_{ex}^T(0)$, $4\pi\beta$, and M_{ex}.

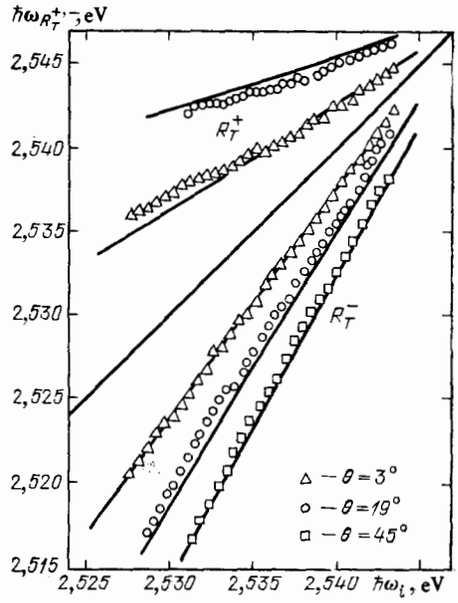

FIG. 17. Dependence of the spectral position of the R_T^+ and R_T^- lines on the photon energy $\hbar\omega_i$ of the exciting radiation at the different angles $\theta = 3.19°$ and 45° in "forward" observation.[130]

One can solve the inverse problem: to reconstruct the polariton dispersion curve from the experimental dependences of the positions of the R_T lines on the photon energy of the exciting radiation. Actually, since one can determine with great accuracy the energies and wave vectors of the photons exciting the semiconductor and the scattered photons, one can determine from the conservation laws (47) the wave vectors and the corresponding energies of the recoil polaritons, and thus construct their dispersion curve. Figure 12 shows by crosses the experimental values of $\hbar\omega_f$ and k_f obtained in the described way when HRS is observed in the back, side, and forward directions. The solid line shows the theoretical dispersion curves for polaritons and longitudinal excitons in CdS that yield the best agreement with the experimental data with the following parameters: $\epsilon_b = 7.5$; $E_{ex}^T(0) = 2.5523$ eV; $\Delta_{LT} = 1.9$ meV. At present the method of determining polariton dispersion by using HRS is not inferior in accuracy to other methods.[118–120,132] The readjustment of the polariton spectrum near a biexciton resonance described below has been studied by this method.

f) Readjustment of the dielectric function near a two-photon biexciton resonance

As is known, the optical properties of a semiconductor (absorption, refraction, etc.) are determined by the complex

dielectric function $\epsilon(\mathbf{k}, \omega)$ that describes the dynamic response of the medium to an external electromagnetic field (the dependence of $\mathbf{k}$ arises in media having spatial dispersion[133]). At low field intensities the induction $\mathbf{D}$ and the electric field $\mathbf{E}$ are related linearly:

$$D_i(\mathbf{k}, \omega) = \sum_j \epsilon_{ij}(\mathbf{k}, \omega) E_j(\mathbf{k}, \omega) = \sum_j [\delta_{ij} + 4\pi\chi_{ij}(\mathbf{k}, \omega)] E_j(\mathbf{k}, \omega).$$

At high intensities of the radiation field the relationship between $\mathbf{D}$ and $\mathbf{E}$ ceases to be linear. In nonlinear optics this situation is taken into account by expanding the polarization $\mathbf{P}$ of the medium as a power series in $\mathbf{E}$. For example, for crystals with an inversion center this expansion has the form

$$\mathbf{P}(\omega) = [\chi^{(1)}(\omega) + \chi^{(3)}(\omega; -\omega, \omega, \omega) |\mathbf{E}(\omega)|^2 + \ldots] \times \mathbf{E}(\omega) = \chi(\omega) \mathbf{E}(\omega).$$

Here $\chi(\omega)$ is the nonlinear permittivity, which depends on $|\mathbf{E}(\omega)|^2$. Analogously one can generalize the expression

$$\mathbf{D}(\mathbf{k}, \omega) = \mathbf{E}(\mathbf{k}, \omega) + 4\pi\mathbf{P}(\mathbf{k}, \omega) = \epsilon_\perp(\mathbf{k}, \omega) \mathbf{E}(\omega)$$

and consider that the dielectric function also depends on the intensity of the electromagnetic field or the density of photons or polaritons.[12]

We shall be interested in the spectral region of two-photon (or two-polariton) excitation of biexcitons. If we know the dependence of the dielectric function on the density of polaritons, we can trace the variation of the optic constants n and $\varkappa$, and also the readjustment of the one-particle polariton spectrum in the spectral region of two-photon biexciton resonance. This type of readjustment was first treated in Ref. 134. A microscopical calculation of the transverse complex dielectric function that depends on the polariton density has been performed in Refs. 135–138 by using the diagram technique for the retarded polarization operators (see also Ref. 139). Without taking up the details of calculations,[140,141] we shall present the resulting expression for $\epsilon_\perp(\mathbf{k}, \omega)$, in which spatial dispersion and the dependence on the density n_p of polaritons near two-polariton resonance of biexcitons have been taken into account:

$$\epsilon_\perp(\mathbf{k}, \omega) = \epsilon_b + \frac{(\epsilon_0 - \epsilon_\infty) E_{ex}^2 [(E_M^* - \hbar\omega_p)^2 - (\hbar\omega)^2]}{[(E_M^* - \hbar\omega_p)^2 - (\hbar\omega)^2][E_{ex}^{*2} - (\hbar\omega)^2] - 4n_p |G_M|^2 E_{ex}^* (E_M^* - \hbar\omega_p)}; \quad (50)$$

Here n_p is the filling number of polaritons of energy $\hbar\omega_p$, G_M is the matrix element corresponding to excitation of biexcitons upon combination of the test photon $\hbar\omega$ with the polariton $\hbar\omega_p$. The spectra of excitons and biexcitons are described by the expressions

$$E_{ex}^* = E_{ex}(0) + \frac{\hbar^2 k_x^2}{2M_{ex}} - i\gamma_{ex}, \quad E_M^* = E_M(0) + \frac{\hbar^2 K^2}{4M_{ex}} - i\gamma_M.$$

Here γ_{ex} and γ_M are the damping constants of excitons and biexcitons, respectively. In the limit of weak excitation levels of the semiconductor ($n_p \to 0$), the nonlinear dielectric function (50) coincides with the dielectric function presented on the left-hand side of (45) with a linear response. When $n_p \neq 0$, singularities arise in the dielectric function of (50) that correspond to resonance absorption at the frequencies.

$$\hbar\omega = \frac{1}{2}[(E_{ex} + E_M - \hbar\omega_p) \pm \sqrt{(E_{ex} - E_M + \hbar\omega_p)^2 + 4E_R^2}]. \quad (51)$$

Here we have $E_R^2 = 4n_p |G_M|^2 E_{ex}(E_{ex} - \hbar\omega_p)$. If the intense excitation in the semiconductor results in a nonequilibrium distribution of excitons with the density n_p ($\hbar\omega_p$) or a quasiequilibrium distribution of excitons (in this case we have $n_p = n_{ex}$, $\hbar\omega_p = E_{ex}$), then, in addition to the ordinary exciton resonance $\hbar\omega = E_{ex}$, this means that one should observe a resonance at the frequency $\hbar\omega = E_M - \hbar\omega_p$ (or $\hbar\omega = E_M - E_{ex}$). If the excitation and the light probing are performed at the same frequency $\hbar\omega_p = \hbar\omega$, which corresponds to the condition for an experiment to observe giant two-photon absorption, then, according to (50), resonance is observed at photon energy values $\hbar\omega = E_M/2$. If one knows the nonlinear dielectric function of (50) and employs the equation $\epsilon_\perp(\mathbf{k}, \omega) = c^2 k^2/\omega^2$ analogous to (45), one can analyze how the one-particle polariton spectrum is readjusted under conditions of two-photon excitation of biexcitons.

Figure 18 shows the spectral dependences of the real (n) and imaginary ($\varkappa$) components of the complex refractive index $n^* = n + i\varkappa = \sqrt{\epsilon_\perp(\mathbf{k}, \omega)}$ calculated by using the dielectric function of (50) for different values of the polariton density n_p and of the biexcitation decay constant

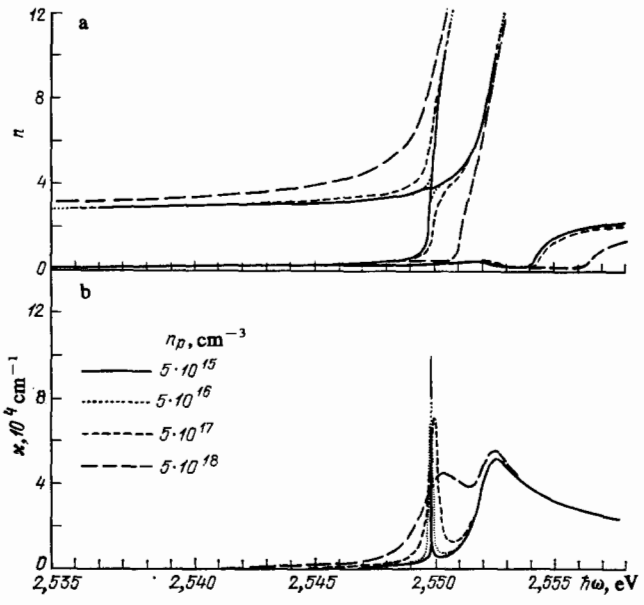

FIG. 18. Spectral dependence of the real (n) and imaginary ($\varkappa$) components of the complex refractive index in the region of exciton and biexciton resonances for different values of the density n_p of polaritons.

$\gamma_M = 3\times10^{-4}$ eV. In the general case with $n_p \neq 0$, three solutions arise for the real component n. This means that three polariton waves should propagate in the crystal at any frequency ω. The greatest splitting of the lower polariton branch is observed near the biexciton resonance $\hbar\omega = E_M/2$. The course of the dispersion of the refractive index of these waves depends both on the polariton concentration n_p of the exciting radiation and on the biexciton decay constant γ_M. The parameter E_R^2 that enters into the expression for $\epsilon_\perp(\mathbf{k}, \omega)$ determines the oscillator strength of the two-photon transition, and hence, the effective magnitude of the corresponding longitudinal-transverse splitting. The splitting between the polariton branches increases with increasing n_p in the region of biexciton resonance. It is known from the theory of excitonic polaritons[94,142] that the effects of spatial dispersion are manifested in optical spectra when the longitudinal-transverse splitting is much larger than the effective damping. When $\gamma \lesssim \Delta_{LT}$, the dispersion curves $n(\hbar\omega)$ become classical. In the region of resonance absorption they show the anomalous course well known in classical crystal optics.[142,143] With increasing excitation level, the ratio E_R/γ_M varies over a broad range. This leads to the transformation of the polariton dispersion curves near biexciton resonance observed in Fig. 18a. At low excitation levels ($n_p \lesssim 10^{15}$ cm^{-3}), the value of the two-photon absorption coefficient $\alpha = 2\varkappa$ is proportional to the density of polaritons, while the half-width of the two-photon absorption lines increases with increasing biexciton decay constant $\hbar\gamma_M$. However, as is implied by Fig. 18b, the half-width of the absorption line is determined not only by γ_M, but it also depends substantially on the polariton density n_p. With increasing excitation level, beginning at a polariton concentration $n_p \approx 10^{15}$–10^{16} cm^{-3}, one observes saturation in the increase in $\varkappa$, while the two-photon absorption coefficient declines at higher n_p. Here the half-width of the two-photon absorption line increases faster than linearly (for constant γ_M). Thus the theory explains the saturation of the increase in the two-photon absorption coefficient and the broadening of the corresponding line with increasing excitation level that have been observed experimentally in crystals of CuCl and CuBr (see Fig. 11).[107,108,144,145]

We note that Figs. 18a, b show the spectral dependences of n and $\varkappa$ for certain polariton densities n_p. In comparing real experimental results with the theoretical curves, one must take into account the fact that the absorption coefficient α, just like the refractive index n, depends substantially in the region of two-photon resonance on the polariton density n_p, which in turn depends nonlinearly on the intensity I_p of the exciting radiation. Namely, we have: $n_p = I_p/\hbar\omega_p v_e$, where $v_e = c/n[1 + (\alpha c/n\gamma_M)]$ is the rate of energy transport in the medium. In the limit of small values of the absorption coefficient α and the decay constant γ_M it goes over into the group velocity for polaritons $v_e \to v_g = d\omega/dk$.[145] Upon scanning the wavelength of the exciting radiation (for fixed intensity I_p) near the biexciton or exciton resonances, the rate v_e of energy transport can vary by several orders of magnitude, which is manifested in a corresponding change in the polariton density. One must also take into account the fact that the intensity of the radiation transmitted through the crystal in the spectral region of biexciton resonance is determined by the equation

$$dI_p(z) = -\alpha(I_p) I_p dz.$$

Here the distribution of the absorption coefficient $\alpha(z)$ is inhomogeneous over the depth of the specimen z.

At present experimental proofs already exist of a variation of the dependence $\alpha(\hbar\omega)$ involving two-photon or induced absorption to form biexcitons in crystals of CuCl, CuBr, and CdS. Comparison of the experimental $\alpha(\hbar\omega)$ relationships with the theoretical calculations enables one to determine not only the biexciton energy $E_M(0)$ in these semiconductors, but also a number of other parameters (the matrix element G_M of the transition, the value of the decay constant γ_M).

It is a more complex experimental problem to measure the variation of the refractive index, which requires using a set of delicate experimental methodologies. Thus, in Refs. 146 and 147 the rotation of the plane of polarization of weak linearly polarized radiation transmitted through a specimen of CuCl and excited by intense circularly polarized radiation with a photon energy $\hbar\omega_p$ was studied. According to the selection rules, creation of biexcitons in the ground state Γ_1 can result only from absorption of light with a circular polarization opposite to the exciting radiation. Analysis of the rotation of the plane of polarization of the probe radiation made it possible to determine the variation of the refractive index $\Delta n \simeq (1$–$3)\times10^{-3}$ as a function of the excitation level and inolving induced absorption at the frequency $\hbar\omega = E_M - \hbar\omega_p$.[12]

It is extremely complicated to perform analogous experiments in uniaxial crystals. Therefore, it has been proposed in a set of studies to measure the variation of the refractive index in CdS to employ the method of deviation of a probe ray by a crystal having the shape of a refractive wedge.[143,148] The measurement of the features in the deviation of the probe ray demonstrated a variation in the refractive index of the order of 10^{-2}–10^{-1} in the spectral range near $\hbar\omega = E_M/2$.

As we have already noted, one of the most exact methods of determining the dispersion curve for polaritons near an exciton resonance is hyper-Raman scattering. A biexciton participates in the HRS process as the intermediate state. Hence the experimental results obtained with HRS enable one to determine small changes in the parameters characterizing the biexciton state. The solid lines in Fig. 19 show the theoretically calculated positions of the HRS line R_T^+ and R_T^- without taking into account the readjustment of the one-particle polariton spectrum (case of extremely small polariton densities $n_p \to 0$). The experimentally measured positions of R_T^+ and R_T^- lines represented by squares, as observed in the forward direction at the angle $\theta = 12°$, differ appreciably from the calculated values as $n_p \to 0$. The dotted lines show the calculated relationships $\hbar\omega_{R_T^{+,-}}$, ($\hbar\omega_i$) with account taken of the readjustment of the polariton spectrum with the following values of the adjustable parameters: $E_{ex}^T(0) = 2.5523$ eV; $\epsilon_b = 7.5$;

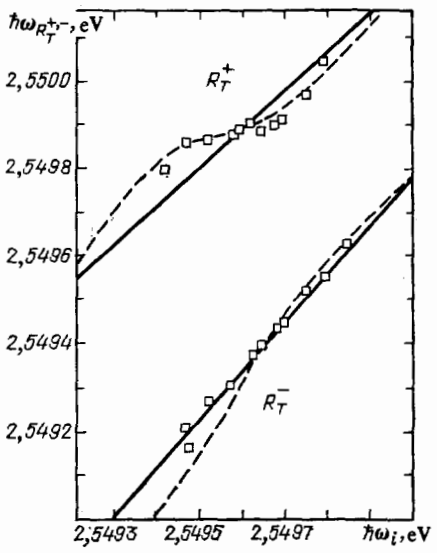

FIG. 19. Experimental and theoretical dependences of the spectral position of the R_T^+ and R_T^- HRS lines in CdS on the photon energy of the exciting radiation $\hbar\omega_i$ in the region of two-photon biexciton resonance without taking into account (solid lines) and with taking into account (dotted lines) the giant two-photon absorption.[126]

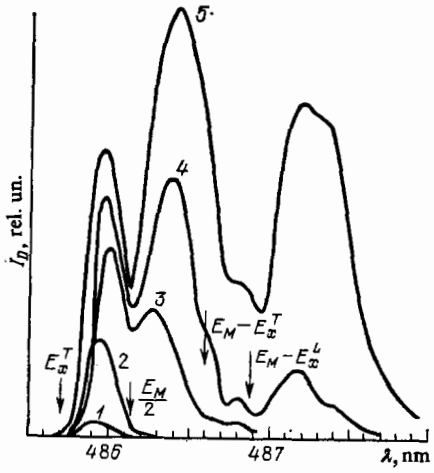

FIG. 20. Spectral dependence of the intensity of radiation diffracted in the first order in the region of two-photon and induced biexciton resonances under different conditions of excitation. 1—1; 2—2.5; 3—10; 4—25; and 5—100 kW/cm^2.

$|G_M|^2 = 10^{-21}$ eV^2·cm^3; $E_M(0) = 5.0992 \pm 2\times10^{-4}$ eV; $\gamma_M = 0.85$ meV. The best agreement between the experimental results and theory was attained by taking into account the dependence of the polariton density on $\hbar\omega_p$ for a fixed intensity of the exciting radiation I_p.

Thus the set of theoretical and experimental studies confirms that "bipolariton" effects are observed in the direct-band semiconductors CuCl, CuBr, and CdS in the region of biexciton two-photon resonance, and are a generalization of the polariton effects near an exciton resonance.

The dependences described above of the refractive index and the two-photon absorption coefficient on the level of excitation for a direct-band semiconductor can be used to observe and study the phenomenon of optical bistability of transmission of plane-parallel specimens of CuCl and CdS.

A theoretical substantiation of optical bistability in the region of a biexciton resonance has been presented in Refs. 149, 138, and 150.

g) Four-wave mixing in the spectral region of two-photon absorption giving rise to a biexciton

The dependence of the refractive index and the absorption coefficient on the level of excitation of a semiconductor can be used for experimental study of the phenomenon of four-wave mixing in crystals of direct-band semiconductors in the spectal region of a biexciton resonance.[151] In this type of experiments two plane beams of laser coherent monochromatic radiation with the wavelength λ and equal intensities I_p converge at the small angle φ on the surface of the specimen under study. Owing to the interference of these beams, the intensity I of the resulting radiation at the surface of the semiconductor has the sinusoidal distribution $I = 4I_p \sin^2(\pi x/d)$ with the period $d = \lambda/\sin\varphi$. With a sufficiently high intensity of the exciting radiation, as a result of the readjustment of the spectral dependence of the absorption coefficient and the refractive index, they prove to be spatially modulated and form an amplitude phase grating (a dynamic holographic grating) with the period d. Each of the exciting beams becomes diffracted by this grating, so that a fan of diffracted rays corresponding to the different orders of diffraction emerges from the excited region. By studying the angular dependences of the intensity of diffracted radiation, one can decide on the spatial distribution of the absorption coefficient α or the refractive index n in the specimen and estimate the diffusion coefficients of excitons and biexcitons in the crystal, as well as their lifetimes and relaxation times.

In particular, one can draw conclusions from the spectral distribution of intensity of the diffracted radiation concerning the propagation of polaritons in the crystal under conditions of two-photon and induced absorption. Figure 20 shows the spectral dependences of the intensity of radiation diffracted in the first order when CdS is excited with two laser radiation beams of differing powers converging at a 1.6° angle. Just as in the case of the spectral dependence of the intensity of hyper-Raman scattering in CuCl[152] and CdS,[126] the intensity of the diffracted radiation is minimal when the crystal is excited strictly in the region of two-photon absorption $\hbar\omega = E_M/2$[153,154] or of induced absorption $\hbar\omega = E_M - E_{ex}$. As has been shown in Ref. 145, this behavior involves the features of the reabsorption of the diffracted radiation in the excited volume of the specimen.

Just like optical bistability, the phenomenon of four-wave mixing can have a practical application in instruments for high-frequency modulation and deflection of laser radiation.

6. CONCLUSION

The experimental and theoretical studies performed in recent years have made possible substantial progress in understanding the structure of excitonic molecules and their optical properties in semiconductors. The variety has been considerably increased both of objects of study in which EMs have been found and of experimental methods of study-

ing these four-particle complexes. Up to now, EMs have been found and studied from all aspects in a number of semiconductors differing in the anisotropy of the spectrum and in the ratio of effective masses of electrons and holes, $\sigma = m_e/m_h$. This enables one to compare the results of the existing calculations of the dependence of the binding energy of EMs on the parameter σ with the most reliable experimental measurements (see Fig. 1). The best agreement with experiment comes from recently performed calculations based on the Monte-Carlo method and the Green's function formalism.[17] We see from Fig. 1 that the quantitative disagreement between theory and experiment is systematic in character. Apparently it involves not only an inexact knowledge of the wave function of the EM. Phonons can make a considerable contribution to increasing the stability of excitonic molecules: deformation—in the case of atomic semiconductors (of the type of Ge and Si) and polarizational—in heteropolar semiconductors (of the type of CuCl, CdS, etc.) Investigation of this little-studied problem would be of undoubted interest.

Other interesting problems remain unsolved. Thus, in many-valley semiconductors of the type of Ge and Si, more complex excitonic molecules can be stable, in which more than two excitons are bound. Such multiparticle structures have no analogs in moleculear spectroscopy. Their stability is implied by calculations[50] and by experimental observations of stable multiexciton complexes involving a shallow impurity in indirect-band semiconductors.[155–157]

The problem has not been studied experimentally of the stability of EMs in the limit of a strong magnetic field in which the Coulomb energy is much smaller than the cyclotron energy. Here it is interesting to know whether the molecular orbitals will be stable in the case of diamagnetic ortho- excitons, and what is the character of the pairwise interaction of these excitons.

In direct-band semiconductors, study of the nonlinear permittivity and the readjustments of the dielectric function near a two-photon resonance involving excitation of EMs remains topical. The prospects of studying other nonlinear-optical phenomena are closely associated with the gigantic nonlinear response of the medium under conditions of two-photon excitation of EMs—multiwave mixing, optical bistability, dynamic holography, etc.

Finally, as we see it, it is of interest to search for excitonic molecules and multiexciton complexes in low-dimensional semiconducting structures, in particular two-dimensional, e. g., in single layer or multilayer heterostructures having quantum wells.[158,159] In such structures multiparticle complexes must be appreciably more stable than in three-dimensional crystalline media.

[1)]We note that, up to now, practically all the studies of EMs in indirect semiconductors have been conducted in silicon and germanium. The only exception is Ref. 25, which reported the observation of EM emission in AgBr. No studies of the properties of EMs in these crystals have yet been carried out.

[2)]In weakly compressed Si crystals having a splitting of the conduction band ΔE_c less than the energy of the smallest intervalley (TA) phonon ($\hbar\Omega_{TA} = 18$ meV), the intervalley relaxation time proves to be much larger than the lifetime of excitons.[48,49] Here "hot" excitons denote those with an electron from the split-off valley.[48] To avoid misunderstanding we note that the thermal energy distribution within the limits of one valley has time to be established in each valley in a time $\tau \ll \tau_{ex}$.

[3)]Information on para- and diamagnetic properties of direct excitons in undeformed Ge is contained in the review of Zakharchenya and Seĭsyan.[52]

[4)]Polarization of an exciton due to motion within strong magnetic fields $\hbar\omega_c \gg$ Ry has been noted and calculated in Ref. 70.

[1]E. A. Hylleraas and A. Ore, Phys. Rev. **71**, 493 (1947).
[2]A. Ore, *ibid.*, p. 913.
[3]M. A. Lampert, Phys. Rev. Lett. **1**, 450 (1958).
[4]S. A. Moskalenko, Opt. Spektrosk. **5**, 147 (1958).
[5]E. Hanamura and H. Haug, Phys. Rep. Ser. C **33**, 210 (1977); C. Klingshirn and H. Haug, Phys. Rep. **70**, 315 (1981).
[6]J. B. Grun, B. Hönerlage, and R. Levy, in: Excitons, eds. E. I. Rashba and M. D. Sturge, North-Holland, Amsterdam, 1982, Chap. 11, p. 459.
[7]V. B. Timofeev, *ibid.*, Chap. 9, p. 349.
[8]E. Hanamura, Solid State Commun. **12**, 951 (1973).
[9]A. A. Gogolin and E. I. Rashba, Pis'ma Zh. Eksp. Teor. Fiz. **17**, 690 (1973) [JETP Lett. **17**, 478 (1973)].
[10]E. I. Rashba, Springer Tracts in Modern Physics **73**, 150 (1975).
[11]N. Nagasawa, T. Mita, and M. Ueta, J. Phys. Soc. Jpn. **41**, 929 (1976).
[12]H. Haug, Festkörperprobleme **22**, 149 (1982).
[13]A. Akimoto and E. Hanamura, Solid State Commun. **10**, 253 (1972); J. Phys. Soc. Jpn. **33**, 1537 (1972).
[14]W. F. Brinkman, T. M. Rice, and J. B. Bell, Phys. Rev. B **8**, 1570 (1973).
[15]J. Adamowski, S. Bednarek, and M. Suffczynski, Solid State Commun. **9**, 2037 (1971); J. Phys. C **11**, 4515 (1978).
[16]E. D. Gutlyansky and V. E. Khartsiev, Solid State Commun. **12**, 1087 (1973).
[17]M. A. Lee, P. Vashishta, and R. K. Kalia, Phys. Rev. Lett. **51**, 2422 (1983).
[18]T. Inui, Proc. Phys.-Math. Soc. Jpn. **20**, 770, 1341 (1938); **23**, 992 (1941); A. Nordsieck, Phys. Rev. **58**, 310 (1940).
[19]R. K. Wehner, Solid State Commun. **7**, 457 (1969).
[20]F. Bassani, J. J. Forney, and A. Quattropani, Phys. Status Solidi B **65**, 591 (1975).
[21]J. R. Haynes, Phys. Rev. Lett. **17**, 860 (1966).
[22]L. V. Keldysh, in: Trudy IX Mezhdunarodnoĭ konferentsii po fizike poluprovodnikov (Proceedings of the 9th International Conference on Semiconductor Physics), Nauka, M., 1968, Vol. 2, p. 1384; in: Éksitony v poluprovodnikakh (Excitons in Semiconductors), Nauka, M., 1971, p. 5.
[23]Ya. E. Pokrovskiĭ and K. I. Svistunova, Pis'ma Zh. Eksp. Teor. Fiz. **9**, 435 (1969) [JETP Lett. **9**, 261 (1969)]; V. M. Asnin and A. A.Rogachev, *ibid.*, p. 415 [JETP Lett. **9**, 248 (1969)].
[24]J. C. Hensel, T. G. Phillips, and G. A. Thomas, Solid State Phys. **32**, 87 (1977).
[25]I. Pelant, A. Mysyrowicz, and C. Benoit a la Guillaume, Phys. Rev. Lett. **37**, 1708 (1976).
[26]V. S. Bagaev, T. I. Galkina, O. V. Gogolin, and L. V. Keldysh, Pis'ma Zh. Eksp. Teor. Fiz. **10**, 309 (1969) [JETP Lett. **10**, 195 (1969)].
[27]V. D. Kulakovskii and V. B. Timofeev, in: Electron-Hole Droplets, eds. L. V. Keldysh and C. D. Jeffries, North-Holland, Amsterdam, 1983, p. 95.
[28]T. M. Rice, Solid State Phys. **32**, 1 (1977).
[29]V. D. Kulakovskiĭ, V. B. Timofeev, and V. M Édel'shteĭn, Zh. Eksp. Teor. Fiz. **74**, 372 (1978) [Sov. Phys. JETP **47**, 193 (1978)].
[30]V. D. Kulakovskiĭ, I. V. Kukushkin, and V. B. Timofeev, *ibid.* **81**, 684 (1981) [Sov. Phys. JETP **54**, 366 (1981)].
[31]V. D. Kulakovskiĭ and V. B. Timofeev, Pis'ma Zh. Eksp. Teor. Fiz. **25**, 487 (1977) [JETP Lett. **25**, 458 (1977)].
[32]B. J. Feldman, H.-h. Chou, and J. W. Wong, Solid State Commun. **26**, 209 (1978).
[33]I. V. Kukushkin and V. D.Kulakovskiĭ, Zh. Eksp. Teor. Fiz. **82**, 900 (1982) [Sov. Phys. JETP **55**, 528 (1982)].
[34]I. V. Kukushkin, V. D. Kulakovskiĭ, and V. B. Timofeev, Pis'ma Zh. Eksp. Teor. Fiz. **32**, 304 (1980) [JETP Lett. **32**, 280 (1980)].
[35]P. L. Gourley and J. P. Wolfe, Phys. Rev. Lett. **40**, 526 (1978); J. P. Wolfe and C. D. Jeffries, see Ref. 27, p. 437.
[36]J. P. Wolfe, in: Proc. 14th Intern. Conference on Physics of Semiconductors, Edinburgh, 1978, p. 367.
[37]G. A. Thomas, E. I. Blount, and M. Capizzi, Phys. Rev. B **19**, 702 (1979).
[38]R. J. Elliott, Phys. Rev. **108**, 1384 (1957).

[39]K. Cho, Opt. Commun. **8**, 412 (1978).
[40]P. L. Gourley and J. P. Wolfe, Phys. Rev. B **24**, 5970 (1981).
[41]V. M. Edelstein, V. D. Kulakovskiĭ, and V. B. Timofeev, see Ref. 36, p. 383.
[42]I. V. Kukushkin, V. D. Kulakovskiĭ, and V. B. Timofeev, J. Lumin. **24-25**, 393 (1981).
[43]V. D. Kulakovskiĭ, I. V. Kukushkin, and V. B. Timofeev, Zh. Eksp. Teor. Fiz. **78**, 381 (1980) [Sov. Phys. JETP **51**, 191 (1980)].
[44]M. L. W. Thewalt and R. Rostworowski, Solid State Commun. **25**, 991 (1978).
[45]A. S. Kaminskiĭ and Ya. E. Pokrovskiĭ, Zh. Eksp. Teor. Fiz. **76**, 1727 (1979) [Sov. Phys. JETP **49**, 878 (1979)].
[46]V. D. Kulakovskiĭ and V. B. Timofeev, Solid State Commun. **33**, 1187 (1980).
[47]M. Taniguchi and S. Narita, J. Phys. Soc. Jpn. **43**, 1262 (1977).
[48]N. V. Alkeev, A. S. Kaminskiĭ, and Ya. E. Pokrovskiĭ, Pis'ma Zh. Eksp. Teor. Fiz. **18**, 671 (1973) [JETP Lett. **18**, 393 (1973)].
[49]V. D. Kulakovskiĭ, I. B. Levinson, and V. B. Timofeev, Fiz. Tverd. Tela (Leningrad) **20**, 399 (1978) [Sov. Phys. Solid State **20**, 230 (1978)].
[50]J. S. Y. Wang and C. Kittel, Phys. Lett. A **42**, 189 (1972).
[51]V. D. Kulakovskiĭ, A. V. Malyavkin, and V. B. Timofeev, Zh. Eksp. Teor. Fiz. 77, 752 (1979) [Sov. Phys. JETP **50**, 380 (1979)].
[52]B. P. Zakharchenya and R. P. Seĭsyan, Usp. Fiz. Nauk **97**, 193 (1969) [Sov. Phys. Usp. **12**, 70 (1969)].
[53]G. E. Pikus, Fiz. Tverd. Tela (Leningrad) **19**, 1653 (1977) [Sov. Phys. Solid State **19**, 965 (1977)]; V. M. Asnin, G. L. Bir, Yu. N. Lomasov, G. E. Pikus, and A. A. Rogachev, Zh. Eksp. Teor. Fiz. **71**, 1600 (1976) [Sov. Phys. JETP **44**, 838 (1976)].
[54]G. L. Bir and G. E. Pikus, Simmetriya i deformatsionnye éffekty v poluprovodnikakh, Nauka, M., 1972 [Engl. Transl., Symmetry and Strain-Induced Effects in Semiconductors, Israel Program for Scientific Translations, Jerusalem; Wiley, N. Y., 1975].
[55]P. D. Altukhov, G. E. Pikus, and A. A. Rogachev, Pis'ma Zh. Eksp. Teor. Fiz. **25**, 154 (1977) [JETP Lett. **25**, 141 (1977)].
[56]V. D. Kulakovskiĭ, A. V. Malyavkin, and V. B. Timofeev, Zh. Eksp. Teor. Fiz. **76**, 272 (1978) [Sov. Phys. JETP **49**, 139 (1978)].
[57]G. L. Bir and C. E. Picus, in: Proc. 7th Intern. Conference on Physics of Semiconductors, Dunod, Paris, 1964, p. 769.
[58]G. Feher, D. K. Wilson, and E. A. Gere, Phys. Rev. Lett. **3**, 25 (1959).
[59]J. C. Hensel and K. Suzuki, Phys. Rev. B **9**, 4219 (1974).
[60]L. D. Landau and E. M. Lifshits, Kvantovaya mekhanika, Nauka, M., 1974 [Engl. Transl., Quantum Mechanics, Pergamon Press, Oxford, 1977].
[61]É. I. Rashba and V. M. Édel'shteĭn, Zh. Eksp. Teor. Fiz. **58**, 1428 (1970) [Sov. Phys. JETP **31**, 765 (1970)].
[62]W. E. Lamb, Phys. Rev. **85**, 259 (1952).
[63]R. S. Knox, Theory of Excitons, Suppl. No. 5 to Solid State Phys., Academic Press, N. Y., 1963 [Russ. Transl., Mir, M., 1966].
[64]T. G. Tratas and V. M. Édel'shteĭn, Zh. Eksp. Teor. Fiz. **81**, 696 (1981) [Sov. Phys. JETP **54**, 372 (1981)].
[65]E. F. Gross, B. P. Zakharchenya, and O. V. Konstantinov, Fiz. Tverd. Tela (Leningrad) **3**, 305 (1961) [Sov. Phys. Solid State **3**, 221 (1961)].
[66]J. J. Hopfield and D. G. Thomas, Phys. Rev. **122**, 35 (1961).
[67]A. G. Samoĭlovich and L. A. Korenblit, Dokl. Akad. Nauk SSSR **100**, 43 (1955).
[68]V. D. Kulakovskiĭ and V. M. Édel'shteĭn, Zh. Eksp. Teor. Fiz. **86**, 338 (1984) [Sov. Phys. JETP **59**, 195 (1984)].
[69]V. E. Bisti, V. M. Edelstein, I. V. Kukushkin, and V. D. Kulakovskiĭ, Solid State Commun. **44**, 197 (1982).
[70]L. P. Gor'kov and I. E. Dzyaloshinskiĭ, Zh. Eksp. Teor. Fiz. **53**, 712 (1967) [Sov. Phys. JETP **26**, 446 (1968)].
[71]H. L. Störmer and R. W. Martin, Phys. Rev. B **20**, 4213 (1979).
[72]V. M. Édel'shteĭn, Zh. Eksp. Teor. Fiz. 77, 760 (1979) [Sov. Phys. JETP **50**, 384 (1979)].
[73]B. S. Razbirin, I. N. Ural'tsev, and G. V. Mikhaĭlov, Pis'ma Zh. Eksp. Teor. Fiz. **25**, 191 (1977) [JETP Lett. **25**, 174 (1977)].
[74]S. A. Moskalenko, Fiz. Tverd. Tela (Leningrad) **4**, 276 (1962) [Sov. Phys. Solid State **4**, 199 (1962)].
[75]L. V. Keldysh and A. M. Kozlov, Pis'ma Zh. Eksp. Teor. Fiz. **5**, 238 (1967) [JETP Lett. **5**, 190 (1967)].
[76]J. M. Blatt, K. N. Böer, and W. Brandt, Phys. Rev. **126**, 1691 (1962).
[77]S. A. Moskalenko, Bose-éĭnshteĭnovskaya kondensatsiya éksitonov i biéksitonov (Bose-Einstein Condensation of Excitons and Biexcitons), Shtiintsa, Kishinev, 1970.
[78]I. V. Kukushkin, V. D. Kulakovskiĭ, and V. B. Timofeev, Pis'ma Zh. Eksp. Teor. Fiz. **34**, 36 (1981) [JETP Lett. **34**, 34 (1981)].
[79]V. B. Timofeev, I. V. Kukushkin, and V. D. Kulakovskiĭ, Physica (Utrecht), Ser. B **117/118**, 327 (1983).
[80]Yu. M. Kagan and G. V. Shlyapnikov, Pis'ma Zh. Eksp. Teor. Fiz. **34**, 358 (1981) [JETP Lett. **34**, 341 (1981)].
[81]L. V. Keldysh and A. N. Kozlov, Zh. Eksp. Teor. Fiz. **54**, 978 (1968) [Sov. Phys. JETP **27**, 521 (1968)].
[82]E. Hanamura, Solid State Commun. **11**, 485 (1972).
[83]A. Frova, P. Schmid, A. Grisel, and F. Levy, *ibid.* **23**, 45 (1977).
[84]V. G. Lysenko and V. I. Revenko, Fiz. Tverd. Tela (Leningrad) **20**, 2144 (1978) [Sov. Phys. Solid State **20**, 1238 (1978)].
[85]V. E. Bisti and A. P. Silin, *ibid.* **20**, 1850 (1978) [Sov. Phys. Solid State **20**, 1068 (1978)].
[86]I.V. Kukushkin, V. D. Kulakovskiĭ, T. G. Tratas, and V. B. Timofeev, Zh. Eksp. Teor. Fiz. **84**, 1145 (1983) [Sov. Phys. JETP **57**, 665 (1983)].
[87]D. Hulin, A. Mysyrowicz, and C. Benoit a la Guillaume, Phys. Rev. Lett. **45**, 1970 (1980).
[88]D. Hulin, A. Mysyrowicz, and C. Benoit a la Guillaume, J. Lumin. **24/25**, 629 (1981).
[89]F. Bassani and M. Rovere, Solid State Commun. **29**, 887 (1976).
[90]V. B. Kadomtsev and V. S. Kudryavtsev, Zh. Eksp. Teor. Fiz. **62**, 144 (1972) [Sov. Phys. JETP **35**, 76 (1972)].
[91]S. T. Chui, Phys. Rev. B **9**, 3438 (1974).
[92]A. G. Zhilich, V. S. Monoson, and B. K. Kyuper, Voprosy kvantovoĭ teorii atomov i molekul (Problems of the Quantum Theory of Atoms and Molecules), Nauka, L., 1982.
[93]G. V. Gadiyak, Yu. E. Lozovik, and M. S.Obrekht, Fiz. Tverd. Tela (Leningrad) **25**, 1063 (1983) [Sov. Phys. Solid State **25**, 613 (1983)].
[94]S. I. Pekar, Kristallooptika i dobavochnye svetovye volny (Crystal Optics and Supplementary Light Waves), Naukova dumka, Kiev, 1982.
[95]F. Henneberger and J. Voigt, Phys. Status Solidi B **76**, 313 (1976).
[96]A. A. Gogolin, Fiz. Tverd. Tela (Leningrad) **15**, 2746 (1973) [Sov. Phys. Solid State **15**, 1824 (1974)].
[97]E. I. Rashba, Fiz. Tekh. Poluprovodn. **8**, 1241 (1974) [Sov. Phys. Semicond. **8**, 807 (1975)].
[98]K. G. Petrashku and P. I. Khadzhi, *ibid.* **9**, 1115 (1975) [Sov. Phys. Semicond. **9**, 734 (1975)].
[99]E. Hanamura, J. Phys. Soc. Jpn. **39**, 1516 (1975).
[100]A. Kuroiwa, H. Saito, and S. Shionoya, Solid State Commun. **18**, 1107 (1976).
[101]G. M. Gale and A. Mysyrowicz, Phys. Rev. Lett. **32**, 727 (1974).
[102]N. Nagasawa, N. Nakata, Y. Doi, and M. Ueta, J. Phys. Soc. Jpn. **38**, 593, 903 (1975); **39**, 987 (1975).
[103]A. Mysyrowicz, A. J. Schmidt, and Y. R. Shen, Solid State Commun. **17**, 523 (1975).
[104]R. W. Svorec and L. L. Chase, *ibid.*, p. 803.
[105]J. Voigt and I. Rückmann, Phys. Status Solidi B **61**, K85 (1974).
[106]V. G. Lysenko and V. B. Timofeev, Fiz. Tverd. Tela (Leningrad) **18**, 1030 (1976) [Sov. Phys. Solid State **18**, 588 (1976)].
[107]Y. Nozue, T. Itoh, and M. Ueta, J. Phys. Soc. Jpn. **44**, 1305 (1978).
[108]J. Puls, I. Rückmann, and J. Voigt, Phys. Status Solidi B **96**, 641 (1979).
[109]F. Bechstedt and F. Henneberger, *ibid.* **81**, 211 (1977).
[110]H. Saito, A. Kuroiwa, S. Kucibayashi, Y. Aogaki, and S. Shionoya, J. Lumin. **12/13**, 575 (1976).
[111]I. Rückmann, V. May, F. Henneberger, and J. Voigt, *ibid.* **24/25**, 593 (1981).
[112]T. Itoh, Y. Nozue, and M. Ueta, J. Phys. Soc. Jpn. **40**, 1791 (1976).
[113]M. V. Lebedev and V. G. Lysenko, Fiz. Tverd. Tela (Leningrad) **25**, 1191 (1983) [Sov. Phys. Solid State **25**, 682 (1983)].
[114]J. M. Hwam, Solid State Commun. **26**, 373 (1978).
[115]S. I. Pekar, Zh. Eksp. Teor. Fiz. **33**, 1022 (1957); **34**, 1176 (1958).
[116]J. J. Hopfield, Phys. Rev. **112**, 1555 (1958).
[117]J. J. Hopfield and D. G. Thomas, Phys. Rev. **132**, 563 (1963).
[118]S. A. Permogorov, V. V. Travnikov, and A. V. Sel'kin, Fiz. Tverd. Tela (Leningrad) **14**, 3642 (1972) [Sov. Phys. Solid State **14**, 3051 (1973)].
[119]V. A. Kisilev, B. S. Razbirin, and N. I. Ural'tsev, Phys. Status Solidi B **72**, 161 (1975).
[120]S. I. Pekar and M. I. Strashnikova, Zh. Eksp. Teor. Fiz. **68**, 2047 (1975) [Sov. Phys. JETP **41**, 1024 (1975)].
[121]V. May and J. Röseler, Phys. Status Solidi B **102**, 533 (1980).
[122]O. Goede, *ibid.* **81**, 235 (1977).
[123]E. Doni, R. Girlanda, and G. Pastori Parravicini, Solid State Commun. **17**, 189 (1975)
[124]Vu Duy Phach, A. Bivas, B. Hönerlage, and J. B. Grun, Phys. Status Solidi B **84**, 731 (1977).
[125]H. Schrey, V.G. Lyssenko, and C. Klingshirn, Solid State Commun. **32**,

897 (1979).
[126]V. G. Lyssenko, K. Kempf, K. Bohnert, C. Klingshirn, and S. Schmitt-Rink, *ibid.* **42**, 401 (1982).
[127]N. Nagasawa, S. Koizumi, T. Mita, and M. Ueta, J. Lumin. **12/13**, 587 (1976).
[128]B. Hönerlage, Vu Duy Phach, A. Bivas, and E. Ostertag, Phys. Status Solidi B **83**, K101 (1977); **86**, 159 (1978).
[129]T. Itoh, Y. Nozue, and M. Ueta, J. Phys. Soc. Jpn. **41**, 713 (1976).
[130]H. Schrey, V. G. Lyssenko, C. Klingshirn, and B. Hönerlage, Phys. Rev. B **20**, 5267 (1979).
[131]H. Schrey, V. G. Lyssenko, and C. Klingshirn, Solid State Commun. **31**, 299 (1979).
[132]G. Winterling and E. Koteles, Solid State Commun. **23**, 95 (1977).
[133]V. M. Agranovich and V. L. Ginzburg, Kristallooptika s uchetom prostranstvennoĭ dispersii i teoriya éksitonov, Nauka, M., 1979 [Engl. Transl., Crystal Optics with Spatial Dispersion, and Excitons, Springer Verlag, Berlin, 1984].
[134]P. I. Khadzhi, S. A. Moskalenko, and S. A. Belkin, Pis'ma Zh. Eksp. Teor. Fiz. **29**, 223 (1979) [JETP Lett. **29**, 200 (1979)].
[135]H. Haug, R. März, and S. Schmitt-Rink, Phys. Lett. A 77, 287 (1980).
[136]R. März, S. Schmitt-Rink, and H. Haug, Z. Phys. Ser. B **40**, 9 (1980).
[137]V. May, K. Henneberger, and F. Henneberger, Phys. Status Solidi B **94**, 611 (1977).
[138]F. Henneberger and V. May, *ibid.* **109**, K139 (1982).
[139]J. Y. Bigot and B. Hönerlage, *ibid.* **121**, 649 (1984).
[140]S. Schmitt-Rink and H. Haug, *ibid.* **113**, K143 (1982).
[141]F. Henneberger and V. May, *ibid.*, p. K147.
[142]M. I. Strashnikova and E. V. Bessonov, Zh. Eksp. Teor. Fiz. **74**, 2206 (1978) [Sov. Phys. JETP **47**, 1148 (1978)].
[143]M. V. Lebedev, V. G. Lysenko, and V. B. Timofeev, Zh. Eksp. Teor. Fiz. **86**, 2193 (1984) [Sov. Phys. JETP **59**, 1277 (1984)].
[144]Y. Masumoto and S. Shionoya, Solid State Commun. **38**, 865 (1981).
[145]S. Schmitt-Rink and H. Haug, Phys. Status Solidi B **108**, 377 (1981).
[146]M. Kuwata, T. Mita, and N. Nagasawa, Solid State Commun. **40**, 911 (1981).
[147]M. Kuwata and N. Nagasawa, J. Phys. Soc. Jpn. **51**, 2591 (1982).
[148]I. Broser, R. Broser, E. Beckmann, and E. Birkicht, Solid State Commun. **39**, 1209 (1981).
[149]S. W. Koch and H. Haug, Phys. Rev. Lett. **46**, 450 (1981).
[150]F. Henneberger and H. Rössmann, Phys. Status Solidi B **121**, 685 (1984).
[151]A. Maruani, J. L. Oudar, E. Batifol, and D. S.Chemla, Phys. Rev. Lett. **41**, 1372 (1978).
[152]Vu Duy Phach, A. Bivas, B. Hönerlage, and J. B. Grun, Phys. Status Solidi B **86**, 159 (1978).
[153]D. S. Chemla, A. Maruani, and E. Batifol, Phys. Rev. Lett. **42**, 1075 (1979).
[154]A. Maruani and D. S. Chemla, Phys. Rev. B **23**, 841 (1981).
[155]A. S. Kaminskiĭ, Ya. E. Pokrovskiĭ, and N. V. Alkeev, Zh. Eksp. Teor. Fiz. **59**, 1937 (1970) [Sov. Phys. JETP **32**, 1048 (1971)].
[156]M. L. W. Thewalt, in: Excitons, North-Holland, Amsterdam, 1982, p. 393.
[157]V. D. Kulakovskiĭ, G. E. Pikus, and V. B. Timofeev, Usp. Fiz. Nauk **135**, 237 (1981) [Sov. Phys. Usp. **24**, 815 (1981)].
[158]R. C. Miller, D. A. Kleinman, A. C. Gossard, and O. Munteanu, Phys. Rev. B **25**, 6545 (1982).
[159]R. C. Miller, J. Appl. Phys. **56**, 1136 (1984).

Translated by M. V. King